NASA CONTRACTOR REPORT

NASA CR-1691

THE DYNAMIC CHARACTERISTICS OF HUMAN SKELETAL MUSCLE MODELED FROM SURFACE STIMULATION

by Jean A. Tennant

Prepared by
STANFORD UNIVERSITY
Stanford, Calif. 94305
for

NATIONAL AERONAUTICS AND SPACE ADMINISTRATION • WASHINGTON, D. C. • FEBRUARY 1971

1. Report No.	2. Government Accession No.	3. Recipient's Catalog No.
NASA CR-1691		

4. Title and Subtitle	5. Report Date
The Dynamic Characteristics of Human Skeletal Muscle Modeled From Surface Stimulation.	February 1971
	6. Performing Organization Code
7. Author(s) Jean A. Tennant	8. Performing Organization Report No. TR No. 6303-1
9. Performing Organization Name and Address Information Systems Laboratory Stanford University Stanford, California 94305	10. Work Unit No.
	11. Contract or Grant No. NGR-05-020-007
12. Sponsoring Agency Name and Address National Aeronautics and Space Administration Washington, DC 20546	13. Type of Report and Period Covered Contractor Report
	14. Sponsoring Agency Code

15. Supplementary Notes

16. Abstract

A mathematical model for the behavior of the muscle group comprised by the biceps and the brachialis was sought taking into account the changes in muscle tension due to the inertia of the moving masses.

The approach involved the postulation of a mechanism composed of a Contractile and a Series Elastic Element. Isotonic and isometric experiments were formulated to allow the explicit characterization of the equations for the postulated mechanism. These experiments involved the artificial stimulation of the muscles via a surface electrode, located at the motor point of the muscle group. In the isotonic experiments, external loads were simultaneously applied to the forearm by means of an electric torque motor. The electric motor was controlled not only as a torque producing device, but also as a regulator to compensate for developing inertial loads during accelerated motions, as well as for the changing geometry of the arm/muscle system. The stimulus waveforms were provided digitally.

17. Key Words (Selected by Author(s))	18. Distribution Statement
Muscle Contraction Muscle Stimulation Automatic Control of Force Application to muscles	1, Muscular System Unclassified - Unlimited

19. Security Classif. (of this report)	20. Security Classif. (of this page)	21. No. of Pages	22. Price*
Unclassified	Unclassified	114	$3.00

*For sale by the National Technical Information Service, Springfield, Virginia 22151

and cat muscles. The principal differences are observed in the neighborhood of equilibrium where larger decelerations are predicted by the model developed in this investigation. Differences in the generality of the models and in their mathematical forms also are discussed. A hypothesis, based on the results of this study and those of previous investigators, is made for the voluntary control of movement; separate functions for the amplitude and frequency of the motor commands from higher centers are assumed. Mathematical constraints for maximum muscle force are also given, showing their dependence on muscle length. It is pointed out, however, that developed muscular force is only dependent on muscle length when it reaches the limits predicted by the constraints.

CONTENTS

CONTENTS (Cont)

ILLUSTRATIONS

TABLES

ACKNOWLEDGMENTS

I am particularly indebted to Professor Gene F. Franklin for his guidance and invaluable suggestions and to Professor Leon Cohen for introducing me to the methods of neurophysiology, for the use of his laboratory, and for his generously given time.

I am also extremely grateful to Drs. Larry J. Leifer and Felix E. Zajac for the valuable discussions regarding the formulation of this investigation and the experimental procedures.

Chapter I

INTRODUCTION

The principal objective of this investigation was to seek a mathematical and descriptive model for the dynamical behavior of human skeletal muscle and to gain a better understanding of its actual mechanism of contraction.

Previous investigations directed toward models of muscle dynamic behavior can be placed in two classes. One group was aimed at isolating the muscle as much as possible and was directed toward a model that would fit the data from single fibers or small fiber bundles. The idea was to begin at an elementary level and work up toward increasingly complex systems. Most of the work involved at least some disturbance of the surrounding muscle tissues by dissection or even complete removal of the muscles from their normal environment. The best known mathematical description resulting from this approach is the one derived by Hill [1].

The second line of investigation was functional rather than physical and sought to explain the external performance of humans at such tasks as flying an airplane or at other skilled tasks. Here, the position of a tracking target usually is considered as the system input and the length of muscles, their velocities and accelerations (eye or limb positions, velocities, and accelerations) as the system output. The objective was a model of total task performance, and the behavior of the muscle entered only indirectly as a modifying function that limited, in some cases, the quality of the response. These experiments, however, represent extensive quantitative data involving action by muscle groups and, by suitably restricting the nature of the task, the dynamic properties of a muscle group can be made a prominent factor in the response. In addition to the dynamic characteristics such experiments uncover, they are extremely valuable because they are performed on an intact normally operating biological system (i.e., no dissection). These studies do not, however, allow specific dynamic elements to be unequivocally localized or associated with specific anatomical structures. A group of investigators led by McRuer [2] follows this approach.

The first method is more fundamental because, hopefully, the resulting model can be associated with the actual biological makeup of the muscles; as a result, this approach was chosen for this investigation. In particular, the hypothesis that a physical system comprised of a contractile and a series elastic element can be used to describe the behavior of human muscle is tested, and a mathematical model for the dynamic characteristics of a muscle group (acting about the elbow and comprised of the biceps and the brachialis) is sought. The above system structure was first postulated by Levin and Wyman [3] and successfully used by Hill, Wilkie, Zajac, and others for single-muscle as well as for small muscle-fiber bundle characterization. The basis for this assumption is that both a single muscle and a "muscle group" are comprised of a mesh of muscle fibers and, therefore, basically are not different in their fundamental structure; instead, the differences are expected to appear in the parameters entering structurally identical equations of motion. The most notable results obtained under this class of investigations have been for frog and cat muscles in vitro and in vivo. Most of these experiments considered an isotonic shortening muscle to characterize its contractile element by applying a constant external load to the muscle throughout its contraction without taking into account the changes in muscle tension due to the inertia of the moving masses. This study investigates the dynamic characteristics of human skeletal muscle in situ, taking into consideration the inertia of the system, and compares the results obtained with those for frog and cat muscles. Another motivation in obtaining a model for the dynamics of human muscle in situ is its more direct applications to two potentially rewarding areas, (1) the biolectric control of prosthesis, where actual muscle signals are used to control movement and (2) the artificial stimulation of paralyzed limbs for patients with an upper motor lesion but whose muscles are in a normal state.

The approach involved the formulation of isotonic and isometric experiments to obtain the explicit characterization of the mathematical equations for the postulated mechanism. The experimental procedure consisted of the artificial stimulation of the muscles via a surface electrode, application of external forces, and recording of the resulting motions. The external forces were applied to the forearm by means of an

electric torque motor that was controlled not only as a torque-producing device but also as a regulator to compensate for developing inertial loads during accelerated motions as well as for the changing geometry of the arm/muscle system. The method of identification used for determining the unknown functions and parameters entering the equations of motion was purely empirical. Curve fitting the pertinent data recorded from the isotonic experiments permitted the explicit characterization of the contractile element. The results of the isometric experiments revealed the steady-state relationship between muscle torque and forearm position and, combined with the results of the isotonic experiments, allowed the characterization of the series elastic element. It should be observed that the above method of postulating a mechanism to represent the kinematic behavior of muscles and explicitly characterizing the dynamical equations needs not provide a unique model. In fact, some trade-off between the complexities of the postulated mechanism and the equations describing its elements possibly could be established.

The experiments on cat and frog muscles were mainly done during neural excitation of maximal amplitudes and tetanic frequencies. Under these conditions, the activation of the muscles is assumed constant and does not enter significantly into the equations characterizing the contractile and series elastic elements. The experiments involved in the investigation here also were conducted strictly under maximal and tetanic conditions. This is considered the logical first step and would allow meaningful comparisons with previous results. "Maximal" stimulus conditions usually imply that the amplitude of the stimulus is large enough to cause all the fibers comprising the muscles to fire; that is, the firing threshold of all muscle fibers is reached or exceeded under maximal conditions. This condition is established easily for experiments conducted in vitro and in vivo, where the peripheral nerve is stimulated distally; however, for our experiments in situ, involving artificial stimulation by an electrode located on the surface of the skin, it is not possible to activate all the muscle fibers of the biceps and brachialis. This is obvious because the maximum torque recorded at the elbow of adults does not exceed 15 ft-lb. The procedure used in the determination and application of the stimulus in this investigation, however, is

such that it can be reasonably assumed that for each subject a fixed number of muscle fibers are activated throughout all the experiments. This is important because, otherwise, an additional variable must be accounted for in the modeling. Essentially, the term "maximal" (as used in this study) denotes the stimulus amplitude necessary to recruit the maximum number of muscle fibers for a given electrode location. The establishment of maximal conditions as defined above is thoroughly described in Chapter IV.

No voluntary activation of the muscles considered was tolerated. Those trials where they occurred were detected easily and discarded. It should be pointed out, however, that the effects of the antagonist (*triceps*) on the observed motions were neglected unless they were caused by voluntary contractions. All subjects who participated in the experiments were normal adults.

A special effort was made to present this material so that it would be technically accessible to both the physiologist and the engineer; that is, the mathematical developments are thoroughly expanded and terminologies normally alien to engineers are avoided as much as possible. The dynamics involved are simple enough to be handled without excessive mathematical rigor and yet without creating ambiguity.

Chapter II is concerned with the postulation of a conceptual model for skeletal muscle, the characterization of the model by equations in general forms, and the development of the equations of motion. In Chapter III, experiments are formulated to allow the explicit mathematical characterization of the contractile and series elastic elements. The experimental methods and results are presented in Chapters IV and V, respectively, and Chapter VI is restricted to the complete characterization of the mathematical model from the experimental data. Chapter VII discusses the results obtained and provides angular velocity-torque curves computed from the model and their transformations into velocity-force curves which are compared with those derived from equations for frog and cat muscles. Differences in the generality of the models and in their mathematical forms are also discussed. A hypothesis, based on the results of this study and those of previous investigators, is made for the voluntary control of movement; separate functions for the amplitude and

frequency of the motor commands from higher centers are assumed. Mathematical constraints for maximum muscle force are also given to show their dependence on muscle length. It is pointed out, however, that developed muscular force is only dependent on muscle length when it reaches the limits predicted by the constraints. The relationships between translational and rotational coordinates are developed in Appendix A, and the muscle-group torque about the elbow is computed. Appendix B evaluates the approximation made in converting the translational equations to rotational forms.

Chapter II

CONCEPTUAL MODEL AND EQUATIONS OF MOTION

In addition to the problems facing the scientist or engineer when attempting to model a man-made system that is qualitatively known (that is, where all the parts comprising the mechanism to be modeled are identifiable and their functions understood), we must contend with a system whose operation at present is not completely known. The actual mechanism by which muscle fibers can contract is not fully understood, and even less understood is the command structure and logic that activate our system of nerves and muscle fibers. In developing a model for human skeletal muscle, we are, therefore, confronted with the problem of postulating a mechanism whose operation describes the behavior of skeletal muscle not only quantitatively but also qualitatively.

A. Conceptual Model Postulated

A mechanical analog to muscle force and kinematic behavior is the model postulated here. It consists of two elements in series: (1) a force generator, whose output depends on muscle excitation and length, in parallel with a damper and referred to as the contractile element and (2) an undamped elastic element called the series elastic element.

Observation of force-velocity curves, as the typical one of Fig. 1, suggested that muscle be modeled as a force generator producing an isometric force P_i in parallel with a viscous element having a coefficient of viscous damping depending on the velocity of the load (contractile element). If a stimulated muscle is held at a fixed length and suddenly is released, however, an instantaneous contraction followed by a more gradual one are observed. A contractile element with viscous damping, as described above, cannot account for the sudden change in the muscle's length; however, an undamped element (series elastic element) in series with the contractile element could describe the above results. This model has been the classical one used by Levin and Wyman [Ref. 3], Hill and others in the study of the frog's sartorius muscles in vitro and, more recently was found by Zajac [Ref. 4] to be applicable in experiments performed on the cat's medial gastrocnemius muscle in vivo. This model

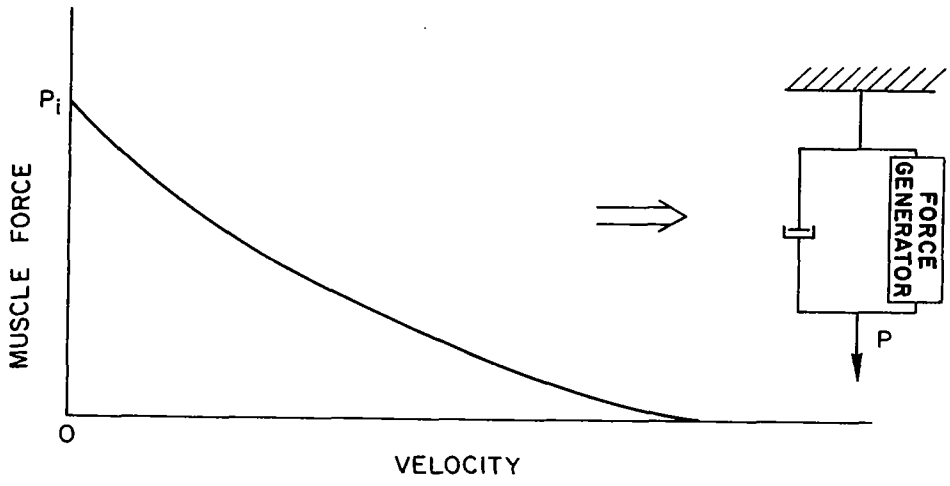

Fig. 1. FORCE-VELOCITY CURVE.

is not unique and, in fact, some trade-off between its complexities and the mathematical equations describing its elements could be established.

The model as postulated in this investigation is illustrated by Fig. 2. The contractile and series elastic elements possibly could be mechanical equivalent elements resulting from actual parallel and series combinations of similar elements in the myofibrils. The elastic element could correspond to the thin filaments and the contractile element to the overlap of both thin and thick filaments. In the schematic representing the contractile element, F denotes the output of the force generator and is represented as a function of both muscle excitation a(t) and of the change in muscle length x_L. It should be noted that the elements making up the contractile and series elastic elements are not implied to be linear; in fact, as this study will demonstrate, they are all nonlinear elements.

B. The Equations in General Form

The general forms of the equations for the assumed model of muscle dynamic behavior and for the arm/muscle/electric motor system involved in the experimental procedures are given in this section. These equations provide insight and guide the experiments required to test the hypothesis on which they are based.

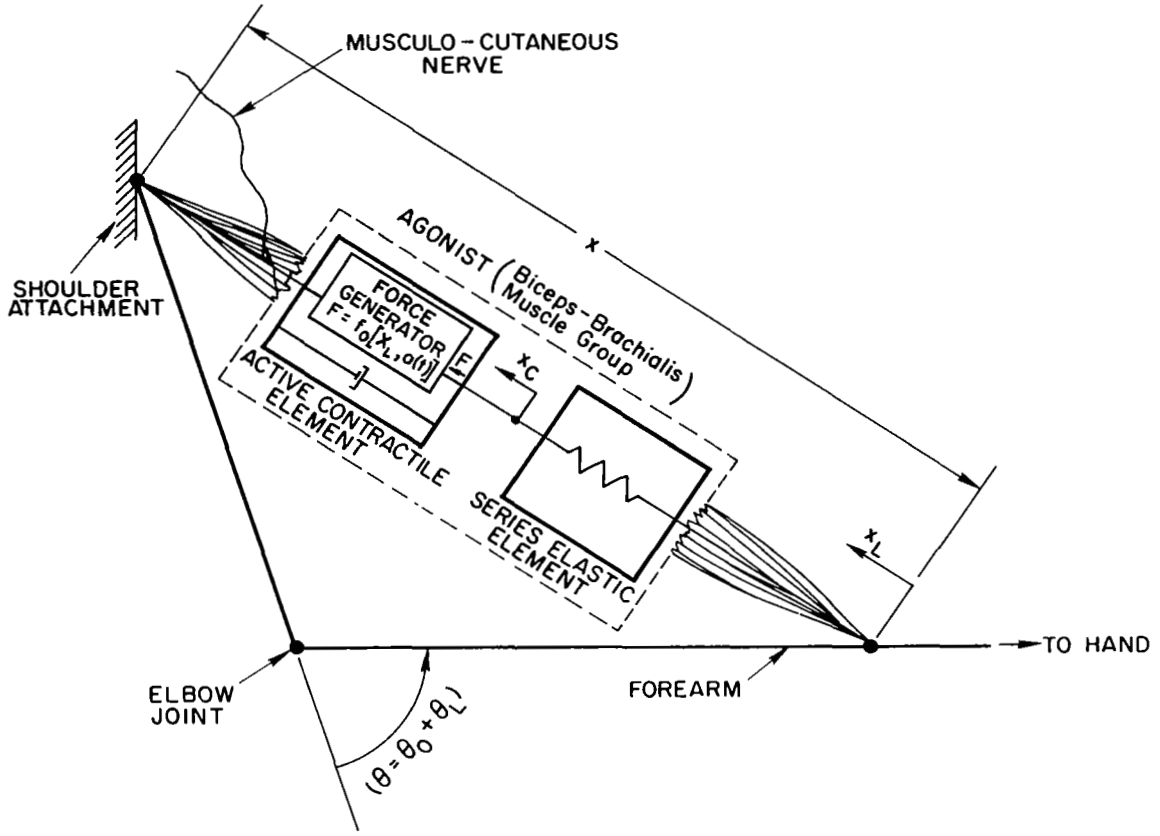

Fig. 2. MODEL OF TORQUE-PRODUCING MUSCLE FOR FOREARM FLEXURE. (Contractile and series elastic elements in series.)

1. Translational Equations and Coordinates for Skeletal Muscle

If the following translational generalized coordinates are defined,

$x_C \equiv$ distance shortened by contractile element from its normal resting length†

† "Normal resting length" of the muscles considered here is defined as that length corresponding to the smallest angle of forearm flexion for completely passive agonist and antagonist and for no tension in the muscle (i.e., for normal resting length a(t), P = 0). θ_0 is approximately 40°.

x_L = distance contracted by muscle group from its normal resting length (i.e., distance moved by attachment point of muscle at forearm from normal resting-length position when shoulder attachment point is fixed)

P = tension in muscle ($P = 0$ at normal resting length)

then, the equations characterizing the series elastic and contractile elements can be represented, respectively, in the following general forms:

$$x_C - x_L = f_1(P) \tag{2.1}$$

and

$$\dot{x}_C = f_2\left[P, x_L, a(t)\right] \tag{2.2}$$

Because muscle fibers generate tension and not compression (the raison d'être of the agonist/antagonist system capability for reversal of movement), it should be noted that a qualitative constraint on the model for contraction originating from the normal resting length of the muscles is

$$|x_C| \geq |x_L|$$

As explained in Chapter I, this investigation was restricted to activation under tetanic and maximal conditions only, such that the neural excitation function $a(t)$ of Eq. (2.2) is a constant throughout the experiments. This function is, therefore, of no further interest and will be dropped from the equations. Its constant value will be considered lumped into the other parameters entering Eq. (2.2) which, therefore, is expressed as

$$\dot{x}_C = f_3(P, x_L) \tag{2.3}$$

2. Conversion of the Translational Equations into Rotational Forms

From the experiments described in Chapter IV, it will be clear that the recording of information is most convenient in rotational rather than translational coordinates; also, it is believed that the mathematical model developed in this study will be more useful and of more direct application if expressed in rotational form. For these reasons, the transformation of the general translational equations into rotational forms is appropriate here. These equations will also form the foundations on which the experiments required to characterize the postulated model will be formulated.

If the following rotational parameters are defined as

θ_0 = angular position of arm, measured from fully stretched position, for normal resting length of muscle group

θ_C = angular displacement of forearm from its normal resting-length position θ_0 corresponding to contraction x_C if series elastic element is assumed fixed in length; i.e., if $x_C - x_L = 0$

θ_L = actual angular displacement of forearm from its normal resting-length position θ_0; i.e., angular displacement corresponding to x_L

then their relationships to the translational coordinates x_C and x_L, as derived in Appendix A, are

$$x_i = \left(\ell^2 + d^2 + 2\ell d \cos \theta_0\right)^{1/2} - \left[\ell^2 + d^2 + 2\ell d \cos (\theta_0 + \theta_i)\right]^{1/2} \qquad (2.4)$$

where $i = C, L$. By using this equation, Eq. (2.1) can be rewritten as

$$\left[\ell^2 + d^2 + 2\ell d \cos (\theta_0 + \theta_L)\right]^{1/2} - \left[\ell^2 + d^2 + 2\ell d \cos (\theta_0 + \theta_C)\right]^{1/2} = f_1(P) \qquad (2.5)$$

The dynamic characteristics of the series elastic element, described by Eqs. (2.1) and (2.5), will not be characterized directly from an experimental procedure; instead, as described in the following chapter,

they will be characterized by making use of the mathematical model for the contractile element that will be developed directly from an experimental investigation. It will be apparent from the results of Chapter VI, however, that the mathematical representation of θ_C is quite complex and, in turn, would render Eq. (2.5), which is the characterization of the series elastic element, very cumbersome and question its usefulness. For these reasons, it is desirable to simplify Eq. (2.5) to the following approximate form,

$$\theta_C - \theta_L = g_1(P) \tag{2.6}$$

A detailed description and validation of this approximation is given in Appendix B.

From the relationships of Appendix A, in particular Eqs. (A.9), (A.10), and (A.12), it is clear that the mathematical model for the contractile element, represented by Eq. (2.3), can be expressed as a general function of muscle-group torque about the elbow and of the rotational coordinates as

$$\dot{\theta}_C = g_2(T_A, \theta_L) \tag{2.7}$$

3. Equations of Motion for Arm/Muscle/Electric-Motor System

In the experimental method, described in Chapter IV, provision is made for the application of an external torque to the forearm by means of an electric motor. A brief description of the system is presented here to identify the interacting forces entering the equation of motion. The forearm is strapped on an aluminum arm attached to the shaft of a torque motor, with the elbow coinciding with the center of the shaft. The subject is seated on a chair whose height can be so adjusted (dental chair) that flexion of the forearm takes place in a horizontal plane. The shoulders are securely strapped to the chair so that attachment points of the muscles at the shoulders can be considered fixed throughout the experiments. A measure of torque is provided by a strain gauge mounted on the aluminum arm. Free-body diagrams of the arrangement

illustrating the pertinent forces acting on the system are shown in Fig. 3. These diagrams are not scaled realistically, and the dimensions are

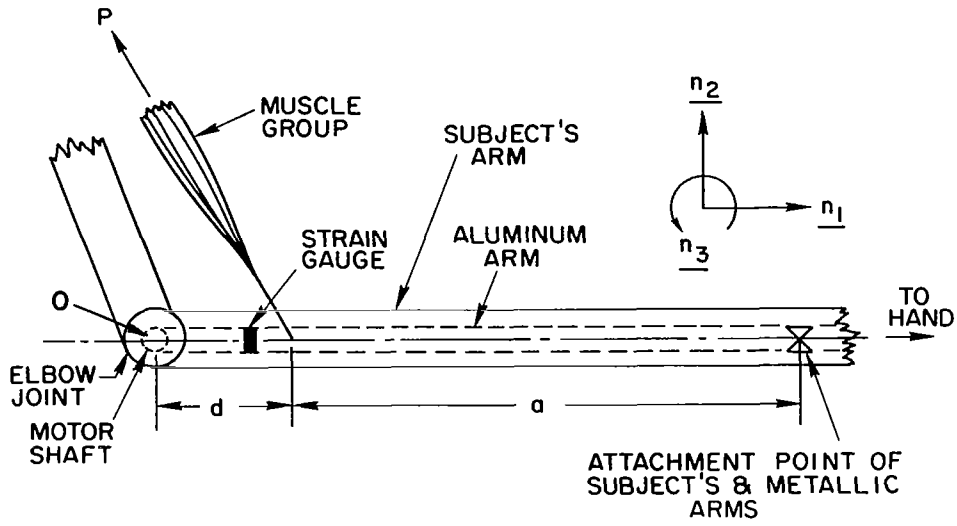

a. Schematic representation

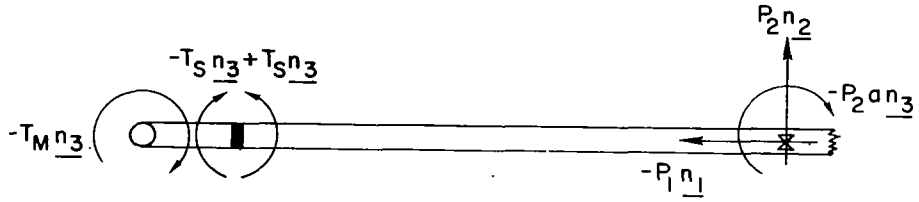

b. Free-body diagram of metallic arm

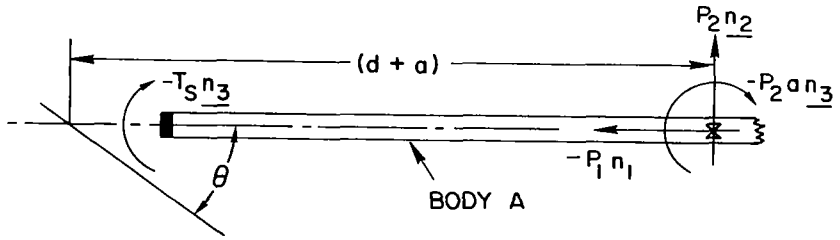

c. Free-body diagram of body A (metallic arm excluding portion between strain gauge and shaft)

Fig. 3. FORCES ACTING ON ARM/MUSCLE/ELECTRIC-MOTOR SYSTEM.

exaggerated where appropriate for illustrative purposes. Note in Fig. 3b that the muscle force P is translated from its point of application at the forearm to the attachment point of the subject's and metallic arms. Addition of the couple $-P_2 a \underline{n_3}$ is necessary for this transformation to be correct. Figure 3c is a free-body diagram of body A, which is that part of the metallic arm excluding the portion between the strain gauge and the shaft. This illustration is given to assist in the derivation of the equation of motion, below, in terms of the strain-gauge torque T_S.

Now, if

$\underline{n_i}$ = set of orthogonal unit vectors, where $i = 1,2,3$

O = rotation point or center of shaft and elbow joint

I_T = moment of inertia of all moving parts (metallic arm + forearm + motor-rotating parts) about O and along unit vector $\underline{n_3}$

I_A = moment of inertia of forearm + body A about O and along $\underline{n_3}$

$\underline{T_M}$ = electric-motor torque about shaft O

$\underline{T_S}$ = torque (bending moment) at strain-gauge location

$\underline{T_A}$ = muscle-group torque about elbow O

P_i = muscle-group force component along n_i vector

d = distance between muscle-group attachment point at forearm and elbow

a = distance between muscle-attachment and metallic-arm-attachment points at forearm

$\underline{H}$ = angular momentum about the fixed point O

$\Sigma \underline{M}$ = summation of the moments of all external forces about O

then the equation of rotational motion

$$\sum \underline{M} = \frac{d}{dt} (\underline{H})$$

for the arm/muscle/electric-motor system is (Fig. 3b)

$$-T_M\underline{n}_3 - P_2 a\underline{n}_3 + \left[(d+a)\underline{n}_1 x \underline{P}\right] = \frac{d}{dt}\left(I_T \dot{\theta}\underline{n}_3\right)$$

or

$$-T_M\underline{n}_3 - P_2 a\underline{n}_3 + \left[(d+a)\underline{n}_1 x (P_1\underline{n}_1 + P_2\underline{n}_2)\right] = I_T\ddot{\theta}\underline{n}_3$$

which becomes

$$-T_M - P_2 a + (d+a)P_2 = I_T\ddot{\theta}$$

and

$$P_2 d = T_M + I_T\ddot{\theta} \tag{2.8}$$

Noting that $\ddot{\theta} = \ddot{\theta}_L$ because $\theta = \theta_0 + \theta_L$, and θ_0 is a constant, and also that $P_2 d$ is the total torque of the muscle group about the elbow T_A because flexion of the arm takes place in a horizontal plane, Eq. (2.8) becomes

$$T_A = T_M + I_T\ddot{\theta}_L \tag{2.9}$$

Similarly, the rotational equation of motion in terms of the strain-gauge torque T_S can be written as (Fig. 3c)

$$-T_S\underline{n}_3 - P_2 a\underline{n}_3 + \left[(d+a)\underline{n}_1 x \underline{P}\right] = \frac{d}{dt}\left(I_A \dot{\theta}\underline{n}_3\right)$$

which reduces to

$$T_A = T_S + I_A\ddot{\theta}_L \tag{2.10}$$

The relationship between muscle-group torque T_A and muscle force P, given by Eq. (A.7), is rewritten here for completeness:

$$T_A = \frac{P\ell d \sin (\theta_0 + \theta_L)}{\left[\ell^2 + d^2 + 2\ell d \cos (\theta_0 + \theta_L)\right]^{1/2}} \tag{2.11}$$

Substituting (2.11) into (2.9) and (2.10), the following equations for muscle force are obtained:

$$P = (T_M + I_T \ddot{\theta}_L) h_5(\theta_L) \tag{2.12}$$

and

$$P = (T_S + I_A \ddot{\theta}_L) h_5(\theta_L) \tag{2.13}$$

where

$$h_5(\theta_L) = \frac{\left[\ell^2 + d^2 + 2\ell d \cos (\theta_0 + \theta_L)\right]^{1/2}}{\ell d \sin (\theta_0 + \theta_L)} \tag{2.14}$$

When expressing the equation of motion in terms of the motor torque T_M rather than the strain-gauge signal T_S (the difference between Eqs. (2.12) and (2.13)), it should be observed that the resulting difference lies in the numerical value for the moment of inertia I_T or I_A. This will play an important role in the implementation of the control system required for the experiments.

C. Summary

The conceptual model postulated for the description of muscle kinematic behavior consists of a contractile element and a series elastic element in series.

The general forms of the equations of motion describing the dynamics of these elements, respectively, are

(a) Translational Coordinates:

$$x_C - x_L = f_1(P) \tag{2.1}$$

$$\dot{x}_C = f_3(P, x_L) \tag{2.3}$$

(b) Rotational Coordinates:

$$\theta_C - \theta_L = g_1(P) \tag{2.6}$$

$$\ddot{\theta}_C = g_2(T_A, \theta_L) \tag{2.7}$$

The equation of motion for the arm/muscle/electric-motor system was developed in terms of both the motor torque T_M and the strain-gauge torque T_S. They were found to differ in the definition of the moments of inertia entering the equations and, therefore, in their numerical values. They are

$$T_A = T_M + I_T\ddot{\theta}_L \tag{2.9}$$

and

$$T_A = T_S + I_A\ddot{\theta}_L \tag{2.10}$$

or in terms of muscle force P,

$$P = (T_M + I_T\ddot{\theta}_L)h_5(\theta_L) \tag{2.12}$$

and

$$P = (T_S + I_A\ddot{\theta}_L)h_5(\theta_L) \tag{2.13}$$

where

$$h_5(\theta_L) = \frac{\left[\ell^2 + d^2 + 2\ell d \cos(\theta_0 + \theta_L)\right]^{1/2}}{\ell d \sin(\theta_0 + \theta_L)} \tag{2.14}$$

This preciseness in the definition and, therefore, in the numerical value used for the moment of inertia, will play an important role in the implementation of the control system required to perform the experiments.

Chapter III

FORMULATION OF EXPERIMENTS

This chapter is devoted to the formulation and implementation of the experiments necessary to characterize the contractile and series elastic elements. The equations developed in the preceding chapter will provide the insight and will form the foundations for formulating the experiments required to test the hypothesis on which they are based. These experiments will be conceived for the characterization of the contractile and series elastic elements in their rotational rather than translational forms. The motivation for this choice stems from the nature of the experiments, where the direct measurements are in angular coordinates. It is also believed that the mathematical model for the muscle group will be of more direct application and usefulness if given in rotational form (e.g., specification of dynamic characteristics for human arm bioelectric prosthesis). Should there be a need, all the data and results obtained can be transformed into translational coordinates using the relationships in Appendix A.

The equations of direct interest here are

$$\theta_C - \theta_L = g_1(P) \tag{2.6}$$

$$\dot{\theta}_C = g_2(T_A, \theta_L) \tag{2.7}$$

which characterize the series elastic and contractile elements, respectively, in rotational form. In these equations, the functions $g_1(\cdot)$ and $g_2(\cdot)$ are only symbolic. It is the purpose of the experimental procedure, based on the hypothesis of these equations, to determine the simplest forms of g_1 and g_2 to explain the data on muscle dynamic behavior.

It is important to realize that, of the generalized coordinates, θ_L (which is the angular displacement of the forearm from its normal resting-length position) is the only one that with its derivatives can be observed and measured experimentally. The coordinate θ_C, which

corresponds to the shortening of the contractile element, cannot be observed directly. An important feature of the experimental procedure, therefore, will be the collection of data to permit the calculation of θ_C and $\dot{\theta}_C$ and the determination of the functions $g_1(\cdot)$ and $g_2(\cdot)$.

A. Characterization of the Contractile Element

The aim in describing the viscous or contractile element of the postulated model is to characterize $g_2(\cdot)$ or Eq. (2.7). The classic approach is through isotonic experiments, that is, experiments under which the muscle force P is kept constant throughout the duration of the experiment. Such experiments allow the determination of θ_C by observing θ_L. This can be established by taking the time derivative of Eq. (2.6)

$$\dot{\theta}_C - \dot{\theta}_L = \frac{\partial g_1(P)}{\partial P} \dot{P} \tag{3.1}$$

and by observing that, when P is constant, $\dot{P}$ is zero and $\dot{\theta}_C = \dot{\theta}_L$, or θ_C only differs from θ_L by a constant. This constant is the angular displacement of the forearm that would correspond to the stretch in the series elastic element from its normal resting length for the particular constant load P_C.

Without referring to the mathematical equations, the above observations can be made by considering only the mechanism of contraction of the postulated model (Fig. 2). If the muscle group is stimulated and if a constant load P_C is applied by the forearm† to the stimulated muscle, the contractile element will shorten, stretching the series elastic element in the process until the latter assumes a tension equal to the load P_C. This phase of the contracting process is isometric; that is, the total muscle length has not changed because the forearm is

† The load is actually applied by a dc electric-torque motor with the forearm strapped to a metallic member that is keyed to the motor shaft, as described in Chapter IV. The load tends to move the forearm toward a stretched position.

still in its initial position. What follows, however, is the isotonic process which is of concern here. Once the tension of the series elastic element has assumed the constant applied load P_C, any further shortening of the contractile element results in no change in the length of the series elastic element but rather in flexion of the forearm; both ends of the series elastic element move in such a way that its total length remains unchanged because its length, corresponding to a unique load P_C, is also unique. As a result, according to the definition of θ_C, the change in θ_C as measured from the beginning of the isotonic process (i.e., from the instant the forearm starts moving) equals θ_L†, and the shortening velocity of the contractile element $\dot{\theta}_C$ equals $\dot{\theta}_L$ which is the actual observed angular velocity of forearm flexion. That is, under isotonic conditions,

$$\theta_C = \theta_L + \theta_{CK} \tag{3.2}$$

and

$$\dot{\theta}_C = \dot{\theta}_L \tag{3.3}$$

where θ_{CK} is the constant angular displacement of the forearm, corresponding to the stretch of the series elastic element from its normal resting length for constant load P_C.

Observation of θ_L and $\dot{\theta}_L$ are, therefore, an indirect but accurate observation of θ_C and $\dot{\theta}_C$ during isotonic experiments and, because θ_C and $\dot{\theta}_C$ are not available for direct measurement, these experiments afford the best data for characterizing Eq. (2.7) describing the contractile element.

B. Idealized Description of Expected Results Based on the Postulated Model

This section is intended to shed more light on the mechanism of contraction described above for the postulated model. For this purpose,

† Similarly, the change in x_C equals x_L during the isotonic process.

expected qualitative time histories and phase-plane plots, based on models developed from previous investigations on frog and cat muscles (Hill and Zajac) are presented. The rationale for presenting phase-plane plots as well as time histories is that they lend themselves well to the analysis of nonlinear data, and the mathematical models for the contractile and series elastic elements, indeed, are expected to be very nonlinear.

Figures 4 and 5 illustrate both the isometric and isotonic processes taking place in the experiments that characterize the contractile element. Reference to the postulated model of Fig. 2, should be made. Motion of the forearm $(\theta_L, \dot{\theta}_L)$ only begins when the series elastic element has been stretched to the length corresponding to the tension P_C; that is, when the developed tension of the series elastic element equals the applied load. During the isotonic process, $\dot{\theta}_C = \dot{\theta}_L$ and θ_C always differs from θ_L by a constant θ_{CK} if the muscle is under constant tension. The magnitude of θ_{CK} depends on the value of the load applied

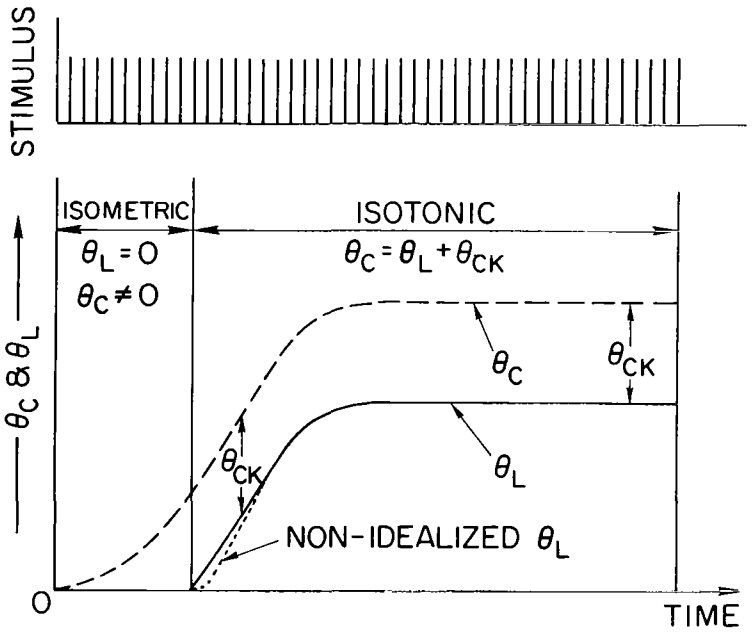

a. Forearm angular position

Fig. 4. QUALITATIVE TIME HISTORIES OF θ_C, θ_L, $\dot{\theta}_C$, AND $\dot{\theta}_L$ FOR POSTULATED MODEL.

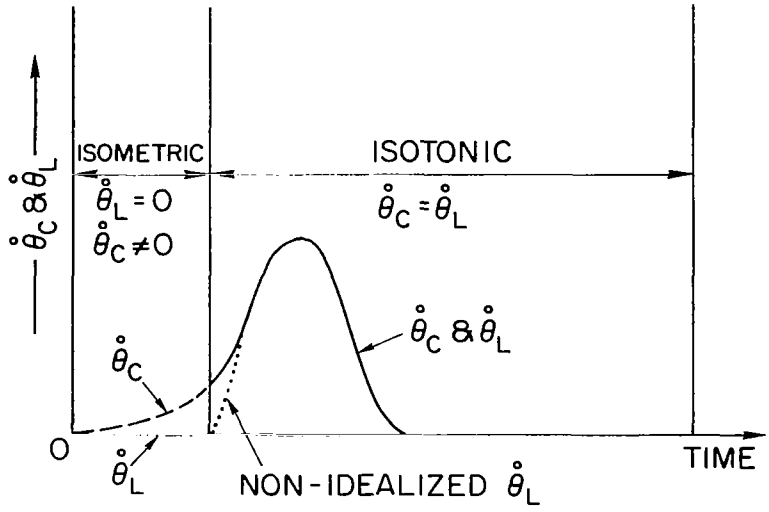

b. Forearm angular velocity

Fig. 4. CONTINUED.

to the forearm. Theoretically, the model suggests an instantaneous finite nonzero value for $\dot{\theta}_L$ at the onset of the isotonic process because $\dot{\theta}_L$ then is equal to $\dot{\theta}_C$, as illustrated in Figs. 4b and 5; however, this also implies an instantaneous velocity of the forearm at the beginning of motion. This cannot occur physically, and dotted lines are drawn to indicate the more realistic shapes of the expected curves under actual physical conditions.

It should be noted that Figs. 4 and 5 are not scaled realistically. For example, the isometric period, which only lasts approximately 75 ms, is greatly exaggerated relative to the total stimulus duration of 1300 ms. Also, the phase-plane plots of Fig. 5 are not quantitatively compatible to the time histories of Fig. 4; they are purely a working description of the postulated model. They will prove very useful, however, in interpreting the experimental data required to characterize the function $g_2(\cdot)$.

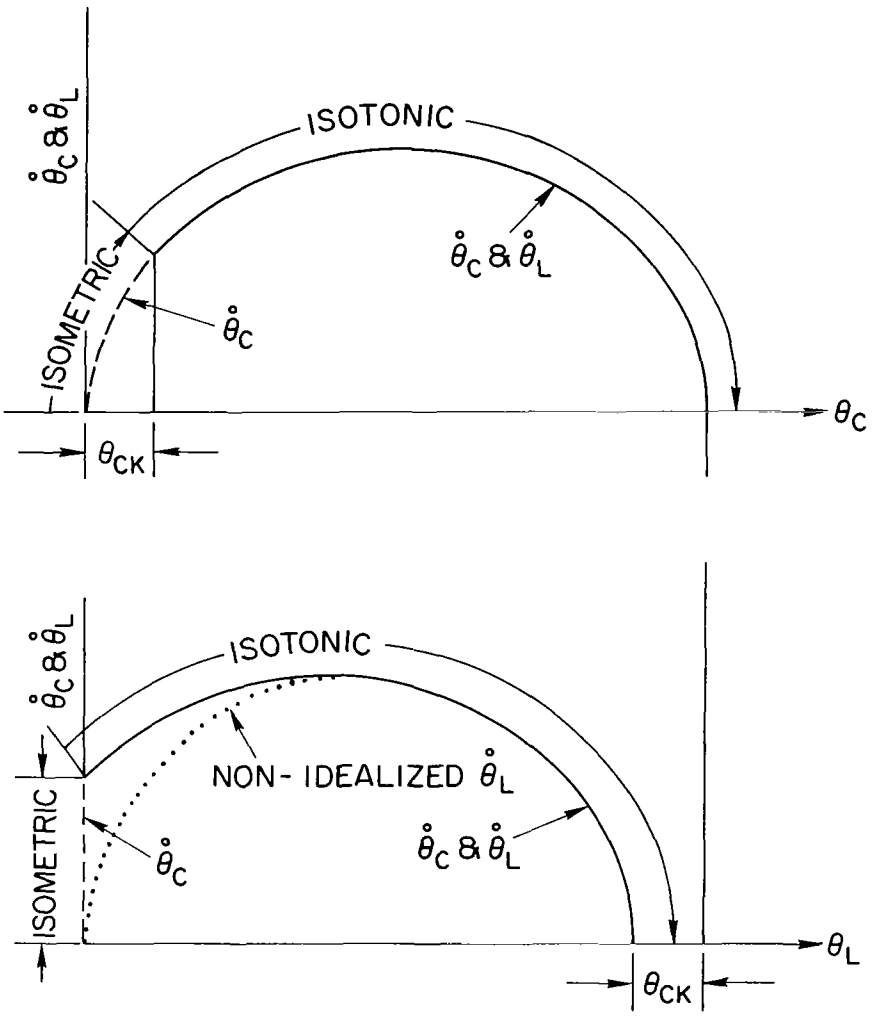

Fig. 5. QUALITATIVE PHASE-PLANE REPRESENTATIONS OF θ_C VS $\dot{\theta}_C, \dot{\theta}_L$ AND θ_L VS $\dot{\theta}_C, \dot{\theta}_L$.

C. Servo-Loop Implementation for Isotonic Experiments

As discussed in the two preceding sections, isotonic experiments, or experiments throughout which the muscle force P remains constant, are necessary to make possible the inference of θ_C and $\dot{\theta}_C$ from measurements of forearm angular position and velocity.

1. The Problem

The method for applying the load to the muscle is by means of a dc torque motor, and the resulting equations governing the flexion of the forearm, developed in Chapter II, were

$$P = (T_M + I_T\ddot{\theta}_L)\, h_5(\theta_L) \tag{2.12}$$

or

$$P = (T_S + I_A\ddot{\theta}_L)\, h_5(\theta_L) \tag{2.13}$$

depending on whether the electric-motor torque T_M computed from the armature current signal, or the torque T_S at the strain-gauge location computed from the strain-gauge signal, is used in the equation of motion. Equation (2.14) defined $h_5(\theta_L)$, as given in Chapter II.

By considering Eq. (2.12)†, it is apparent that, if an experiment is to be isotonic (if P is to remain constant throughout), the right-hand side of the equation must be kept constant. The following two significant difficulties, however, complicate such isotonic experiments.

(a) The angular acceleration of the forearm deflection $\ddot{\theta}_L$ can be assumed by no means to be constant throughout such experiments; from the observations of past investigators, it is not. Therefore, unless the product $I_T\ddot{\theta}_L$ can be neglected (unless the inertia of the system I_T is negligibly small), some adjustment to compensate for the variations in $I_T\ddot{\theta}_L$ must be made for isotonic conditions to exist.

(b) The function $h_5(\theta_L)$ plotted in Fig. 6 for the range of θ_L is not constant because of the changing geometry of the arm/muscle system during forearm flexion. In essence, $h_5(\theta_L)$ accounts for the changing length of the moment-arm vector $\underline{q}$ in the equations of motion (see Fig. 41 in Appendix A).

† The discussions that follow in reference to Eq. (2.12) also apply analogously to Eq. (2.13).

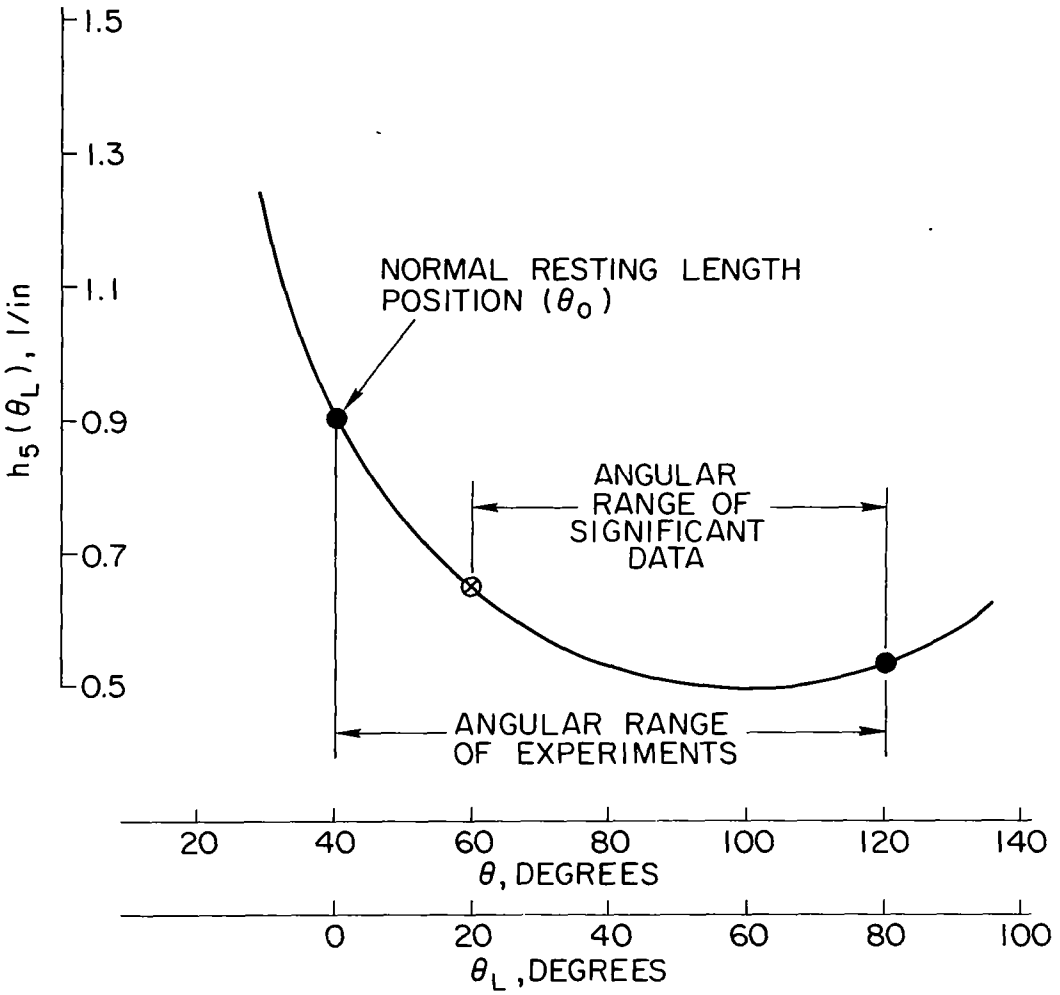

Fig. 6. $h_5(\theta_L)$ VS θ AND θ_L. (ℓ = 10 in.; d = 2 in.)

The inertia term I_T is, therefore, the only constant on the right-hand side of Eq. (2.12) because no change of mass occurs during the experiments. The applied load (electric-motor torque) T_M is the only other term that can be controlled easily and kept constant (by applying a constant input current to the motor), if the hope was to keep every individual parameter on the right-hand side of the equation constant. However, T_M will not be kept constant, and it is this flexibility that will permit true isotonic experiments to be conducted. The value of T_M will be controlled in such a way that it compensates for the changes in the values of $\ddot{\theta}_L$ and $h_5(\theta_L)$. This will be accomplished by making use of

some feedback control logic in driving the torque motor, as discussed later in this section.

Previous investigators surmounted the first difficulty, involving variations in the term $I_T\ddot{\theta}_L$[†], by simply ignoring it. They were able to do so because they dealt with low-inertia systems and studied muscles such as the sartorius of frog and the medial gastrocnemius of cat, which have small masses compared to the biceps-brachialis group. Furthermore, external forces applied to these muscles being small allowed the design of low-inertia systems (low-inertia springs) for the application of these forces. In conclusion, the total inertias involved in their experiments (the terms analogous to I_T) were negligibly small. However, some transient high-frequency oscillations due to the inertia of the systems could still be detected in their results. These inertia effects somewhat disrupted the experimental results, but extrapolation of the data permitted useful conclusions to be drawn. For the study of the biceps-brachialis muscle group presented here, it was not possible to tolerate or to ignore these inertia effects.

The second difficulty, involving the scalar variable $h_5(\theta_L)$, did not occur in previous investigations. These experiments were performed in vitro and in vivo, allowing direct measurements of the shortening muscles in translational motions rather than measurements of limbs in rotational motions. No limb/muscle geometry entered the problem.

2. The Solution

The method of solution adopted in solving the two problems confronted in running isotonic experiments was to take advantage of the available control of the torque motor. This was done by using it not only as a torque-producing device to apply the load T_M to the forearm but also using it as a regulator in adjusting the value of T_M to compensate for the variables $I_T\ddot{\theta}_L$ and $h_5(\theta_L)$ in such a way as to keep the right-hand side of Eq. (2.12) constant.

[†] To be more precise, reference should be made to the terms "analogous to $I_T\ddot{\theta}_L$" (rather than to $I_T\ddot{\theta}_L$ by itself) if the equations of motion for the systems involved in the previous investigations were formulated analogously.

The servo-control logic of Fig. 7 illustrates this solution. The constant input voltage V_i, corresponding to the desired constant force P_i in the muscles for a given isotonic trial, is kept constant

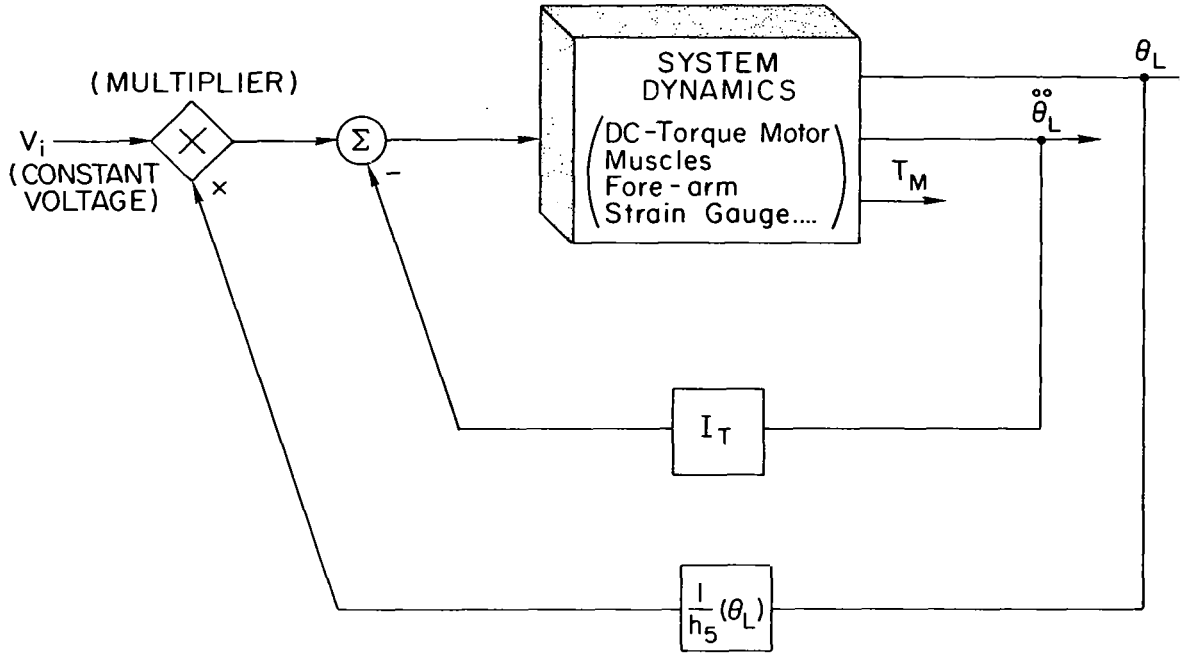

$$P = (T_M + I_T\ddot{\theta}_L)\, h_5(\theta_L)$$

$$h_5(\theta_L) = \frac{\left[\ell^2 + d^2 + 2\ell d \cos(\theta_0 + \theta_L)\right]^{1/2}}{\ell d \sin(\theta_0 + \theta_L)}$$

Fig. 7. FEEDBACK CONTROL LOOPS REQUIRED FOR COMPENSATION OF INERTIA AND CHANGING GEOMETRY OF ARM/MUSCLE SYSTEM DURING ACCELERATED ISOTONIC MOTIONS.

throughout the experiment. The inner loop, involving the sensing of the forearm angular acceleration $\ddot{\theta}_L$ and the feeding back of the negative product $-I_T\ddot{\theta}_L$ to the summing junction, provides the solution for difficulty (a) by precisely compensating for the variable product $I_T\ddot{\theta}_L$. The outer loop, resulting in the feeding back of the inverted function $1/h_5(\theta_L)$ to a multiplier as shown, accounts for difficulty (b) which

is the changing geometry of the arm/muscle system during flexion of the forearm. It should be observed that, without the outer loop, the system indicated by Fig. 7 would provide experimental trials with constant muscle torque rather than constant muscle force P; the right-hand side of Eq. (2.9) would have been kept constant during the trial rather than the right-hand side of Eq. (2.12).

Figure 8 is a block diagram of the system that was actually used in carrying out the isotonic experiments. The additional loop introduced (the feeding back of torque using the strain-gauge signal T_S) is solely for the purpose of improving the dynamic response of the

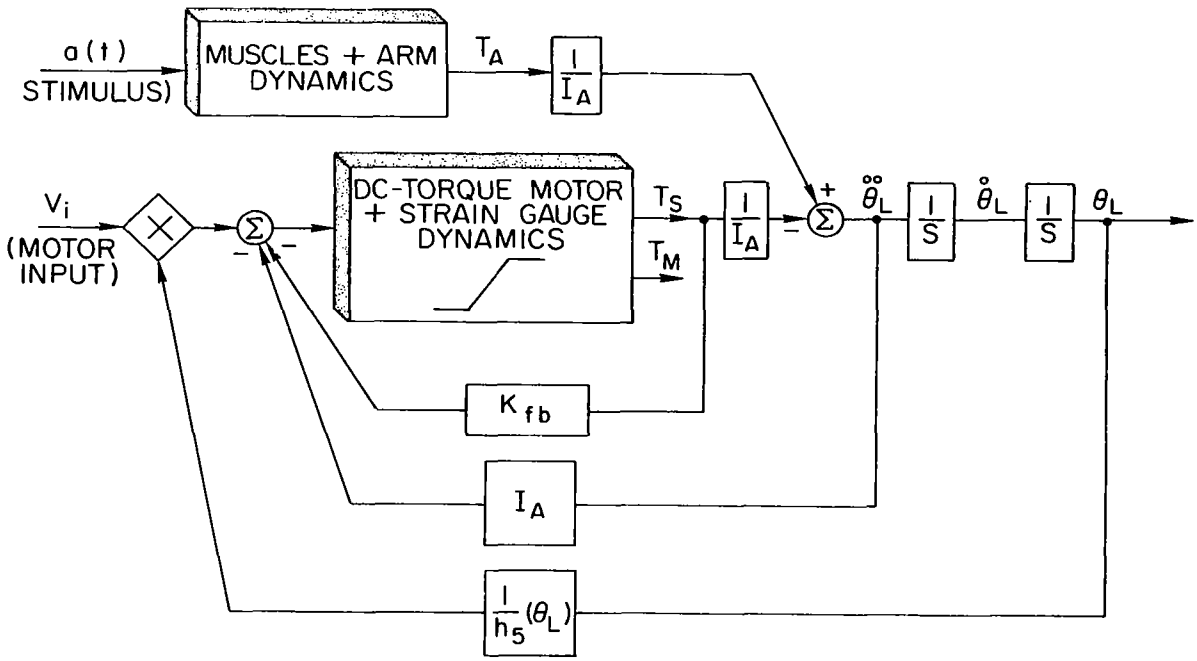

Fig. 8. BLOCK DIAGRAM OF ARM/MUSCLE/ELECTRIC-MOTOR SYSTEM FOR ISOTONIC EXPERIMENTS USING STRAIN-GAUGE SIGNAL.

torque motor. The use of this loop is an application of the basic concept of "feedback," where the value for the gain K_{fb} was chosen to optimize the frequency response of the torque motor, that is, to maximize its bandwidth within acceptable stability margins. The net effect of this loop resulted in a more accurate following of the input command by

the torque output of the motor and a decreased sensitivity of the system to external disturbances. As pointed out, the output signal T_S (strain-gauge signal) rather than T_M (armature-current signal) was used to implement this loop. This choice was based experimentally on the quality of these two signals. The armature-current signal, from which T_M is derived, was "noisier" than the strain-gauge signal used to compute T_S.

Another deviation of the system of Fig. 8 from that of Fig. 7 is in the numerical value of the moment of inertia I_A used in the feedback loop. Because the torque output signal considered in Fig. 8 is T_S, the pertinent equation of motion governing the flexion of the forearm is Eq. (2.13) rather than (2.12); that is, the system actually used in the experiments (Fig. 8) maintains the right-hand side of Eq. (2.13) constant throughout each trial. All the discussions in this section relative to Eq. (2.12) are completely analogous to Eq. (2.13).

D. Characterization of the Series Elastic Element

The aim in characterizing the series elastic element is to write the equation describing its behavior, namely,

$$\theta_C - \theta_L = g_1(P) \tag{2.6}$$

in an explicit form where the symbolic function $g_1(\cdot)$ is fully described.

The contractile element was characterized directly and entirely from the results of the isotonic experiments; however, the results of both the isotonic experiments and a new set of purely isometric experiments will be used to characterize the series elastic element. The pertinent data from the isometric experiments will be the time histories of muscle-group torque about the elbow T_A for different muscle lengths.

Under isometric conditions, where the total muscle length remains fixed throughout the experiment or, for the case considered here, where both the shoulder and the forearm are restricted from moving,

$$T_A = T_S \tag{3.4}$$

This is observed from Eq. (2.10) because the angular acceleration $\ddot{\theta}_L$ is zero. Therefore, by fixing the metallic member on which the subject's arm is attached and by stimulating the muscle group, the time history of the torque T_A of the muscles about the elbow can be obtained by calculating T_S from the observed strain-gauge signal. Consequently, if the length of the muscle, or the position of the forearm, is varied for each trial, the forearm angular position as a function of the steady-state muscle torque can be established easily from the resulting data, namely

$$\theta_L = r(T_A) \tag{3.5}$$

Using these results, Eq. (2.7) can be expressed in terms of only two dependent variables; thus, by substituting Eq. (3.5) into (2.7) for θ_L,

$$\dot{\theta}_C = g_3(T_A) \tag{3.6}$$

Integration of (3.6) yields

$$\theta_C = \int_0^t g_3(T_A)\, dt \tag{3.7}$$

where t = real time.

Finally, by making use of Eqs. (3.5) and (3.7), the characterization of the series elastic element by Eq. (2.6) becomes, for steady-state conditions,

$$\theta_C - \theta_L = \int_0^t g_3(T_A)\, dt - r(T_A) \tag{3.8}$$

subject to the constraint $\theta_L = r(T_A)$ of Eq. (3.5).

Again, the isometric experiments must be carried out with the arm flexed in a horizontal plane if the strain-gauge measurements are to give a true observation of T_A as defined in this study.

E. Summary

To determine the simplest explicit forms for $g_1(\cdot)$ and $g_2(\cdot)$ in Eqs. (2.6) and (2.7) which characterize the series elastic and contractile elements, two sets of experiments, isotonic and isometric, were formulated.

Under isotonic conditions, that is, when muscle tension P is kept constant,

$$\dot{\theta}_C = \dot{\theta}_L \tag{3.3}$$

and

$$\theta_C = \theta_L + \theta_{CK} \tag{3.2}$$

and because the angular displacement of the forearm θ_L is the only generalized coordinate that, with its derivatives, can be measured experimentally, isotonic conditions are necessary to permit the inference of θ_C and $\dot{\theta}_C$ from measurements of θ_L and $\dot{\theta}_L$. These conditions were obtained by using an electric motor not only as a torque-producing device to apply the load to the muscles but also as a regulator (Fig. 8) to compensate for the inertia of the system during accelerated motions [$I_A\ddot{\theta}_L$ in Eq. (2.13)] as well as for the changing geometry of the arm and muscles during flexion of the forearm $h_5(\theta_L)$ in Eq. (2.13). Such compensations were necessary to maintain the right-hand side of Eq. (2.13) constant, that is, to keep P constant and the experiments isotonic. These isotonic experiments, alone, provide enough information to completely characterize the contractile element.

A set of isometric experiments providing time histories of muscle-group torque about the elbow T_A for different muscle lengths permits the explicit description of the function $r(\cdot)$ in the steady-state torque equation, Eq. (3.5).

These results allow Eq. (2.7) to be expressed in terms of only two dependent variables by substituting (3.5) for θ_L. Integration of the resulting equation yields Eq. (3.7).

The series elastic element is then characterized, for steady-state conditions, from the results given by Eqs. (3.5) and (3.7) and Eq. (2.6), thus

$$\theta_C - \theta_L = \int_0^t g_3(T_A)dt - r(T_A) \tag{3.8}$$

subject to the constraint given by (3.5).

The results of both the isotonic and isometric experiments are, therefore, used to describe the series elastic element.

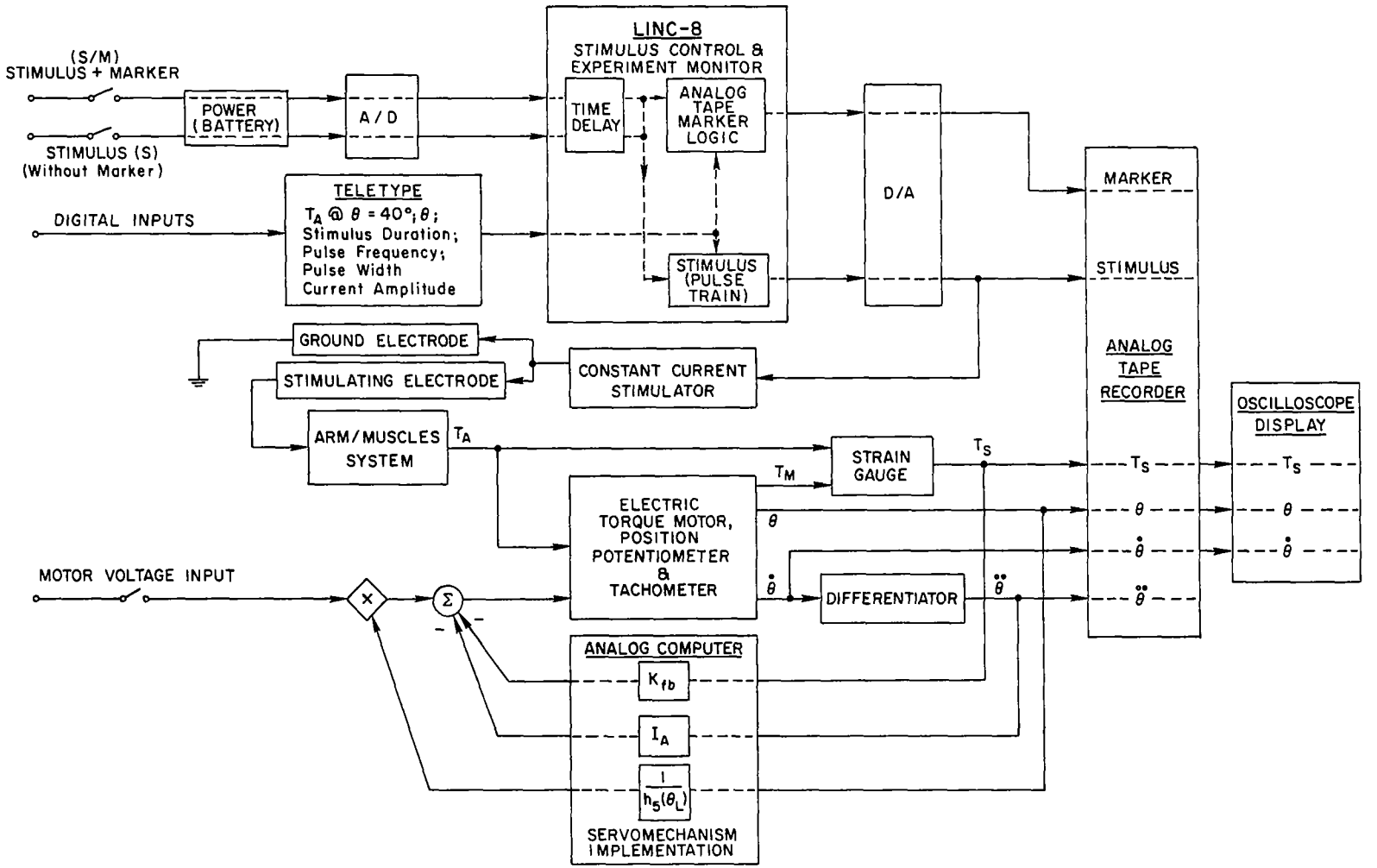

Fig. 9. BLOCK DIAGRAM OF EXPERIMENTAL SYSTEM.

Fig. 10. EQUIPMENT USED IN CONDUCTING EXPERIMENTS.

in the foreground. The stimulator, amplifiers for the strain gauge, the analog computer, and the patch panel where most of the system connections were made appear in the background. Additional equipment included the digital computer, the tape recorder, and the oscilloscope.

A. Method of Stimulation

Excitation of the muscle group was performed by a stimulating electrode held externally on the skin surface at the motor point location. The skin was not broken.

1. Electrodes Used

The stimulating electrode was a 1 in. copper disk, soldered to the electrical lead. A thin felt pad soaked in saline was attached to the surface of the electrode in contact with the skin to provide more

uniform current conduction. This electrode was selected from preliminary experiments where various shapes and sizes were considered. Although the motor point is well defined for any one angular position of a joint (or muscle length), it shifts during motion of the joint because of the muscle movement relative to the skin [Ref. 5]. The motor point for the flexor of the forearm was found to lie within an area approximately 1 in. in diameter from full extension to full flexion of the elbow joint. This suggested the use of an electrode that would cover this area. For the muscle group considered, the motor point for an adult subject of average size lies within 3 to 4 in. from the elbow joint on top of the muscles.

Possibly the most difficult and critical part of the experiments was the determination of an efficient method of applying the stimulating electrode at the motor point of the muscles. The level of muscle excitation, for the same current input, is not only a function of the location of the electrode but also of the pressure between the electrode and the arm. Several devices were tried, including a 1/2 in. rubber band, a "clamping" mechanism resembling a C-clamp with the electrode mounted on the threaded member, and a spring-loaded clamp. All these devices allowed adjustments in the pressure between electrode and arm. The rubber-band attachment gave the worst results, while the spring-loaded clamp was the most encouraging; however, with practice and experience, the most consistent results were obtained by holding the electrode manually, as shown in Fig. 11. The electrode is held between the fore and middle fingers, and the thumb is placed on the outside of the subject's arm to provide the balancing pressure.

Neither the location nor the shape of the ground electrode appeared to have much effect on the effectiveness of stimulation. The one selected was a flat piece of rectangular metal (EEG electrode) and was attached to the forearm by means of a wide rubber band. Electrode jelly was applied on the surface in contact with the skin for better conduction.

Fig. 11. METHOD OF STIMULATION.

2. Stimulus Waveform Used

The waveforms used as stimuli were dc rectangular pulses. Three parameters are required to characterize a dc pulse train: amplitude I, frequency or number of pulses/sec ω, and pulsewidth D. As noted above, all the experiments were conducted under stimuli conditions producing both tetanic and maximal contractions; that is, the frequency of the stimulus was high enough for the individual muscle twitches corresponding to each pulse to overlap into a smooth muscle contraction (tetanus), and the amplitude or width of the pulses were large enough to exceed the firing threshold of all the motor units involved (maximal).

The values required for the above parameters were chosen from preliminary experiments in which they were varied individually. Tetanus seemed to be reached for pulse frequencies above 20/sec, although some ripple in the developed torque (strain-gauge signal) could be observed

for frequencies below 60 pulses/sec. For this reason, most experiments were run at frequencies between 60 and 75 pulses/sec. A given torque can be achieved by holding either I or D fixed and by varying the other parameter. The pulsewidth D was usually held to a fixed value (between 0.5 and 0.8 ms), and the current amplitude I was used as the control signal to achieve maximal stimulation. This was accomplished by gradually increasing I and recording the developed torque until any further increase in I would not be accompanied by an increase in torque. The values of I required for maximal conditions ranged between 7 and 8 mA.

B. Method of Load Application

The loads required for the isotonic experiments were provided by a dc torque motor (Inland Motors MG-5111A) that was shock-mounted in a steel cage. Feedback sensors included a self-contained tachometer and bottom- and top-mounted potentiometers on the dc motor shaft. As previously noted, the torque motor was controlled not only to produce the required loads but also as a servomechanism to compensate for developing inertial loads during accelerated motions and for the changing geometry of the arm/muscle system. This control system was implemented on an analog computer, according to the representation of Fig. 12.

1. Angular-Acceleration Feedback Loop

Angular acceleration of the forearm was obtained by differentiating the tachometer signal, as indicated by the differentiator/filter circuit of Fig. 12. The linear representation of this system is given by the following transfer function:

$$\frac{y}{u}(S) = \frac{-RCS}{(RCS + 1)^2} \qquad (4.1)$$

where

u ≡ differentiator input

y ≡ differentiator output

S ≡ Laplace transform operator

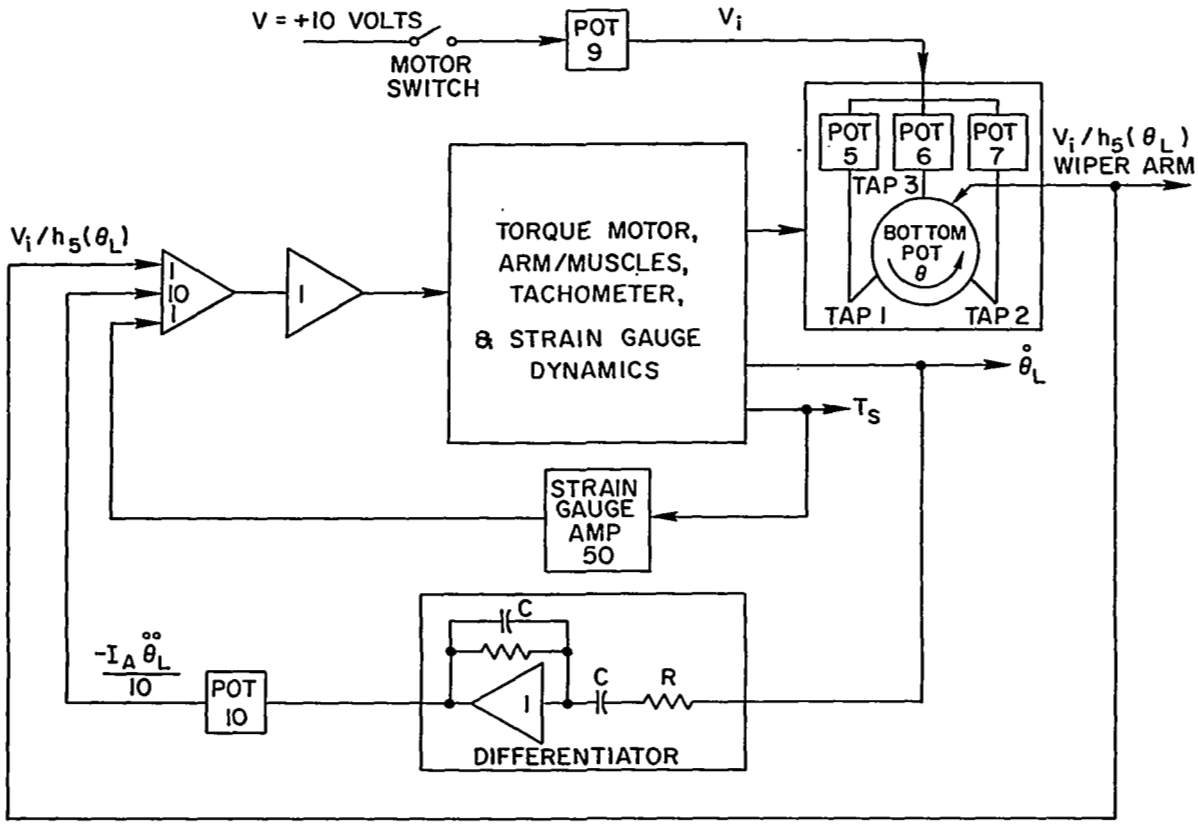

Fig. 12. CONTROL-SYSTEM IMPLEMENTATION USING ANALOG COMPUTER.

R ≡ resistor

C ≡ capacitor

and, for the values of R and C used and presented in Table 1, the first-order filter has a breakaway frequency at 48 cycles/sec; that is, in the low-frequency range of interest, the tachometer signal is differentiated while high-frequency disturbances or noise are attenuated or filtered. The moment of inertia I_A was computed using the approximate mass given in Table 1 (percent of total body weight) for the hand and forearm; the values of I_A and of the other parameters were needed to determine the setting of pot No. 10 in the acceleration feedback loop of Fig. 12.

Table 1

VALUES OF PARAMETERS FOR ANALOG-SERVO IMPLEMENTATION

Parameters	Units	Numerical Values
$\frac{\text{Hand \& Forearm} \times 100}{\text{Total Body Weight}}$	percent	3.45
I_A	ft-lb-sec^2	0.06
C	mF	0.033
R	ohm	100 K
Tachometer Signal	V-sec/rad	2.8
Motor Torque (open loop)	ft-lb/V	12.5
Pot No. 10 Setting	---	0.54

2. Nonlinear-Position Feedback Loop

The nonlinear-position feedback loop was implemented by making use of the potentiometer mounted at the bottom of the motor shaft. The voltages at the "taps" of the potentiometer were controlled from the analog computer to provide the desired $1/h_5(\theta_L)$ feedback function. The settings of pot Nos. 5, 6, and 7 determine $1/h_5(\theta_L)$, while the setting of the control pot No. 9 determines the external load applied to the forearm (the torque applied by the motor). Their relationship is given in Table 2.

Table 2

MOTOR TORQUE VS CONTROL-POT SETTING FOR $\theta = 40^{\circ}$†

Control-Pot Setting (No. 9)	.107	.159	.211	.274	.380	.462	.581	.691
Motor Torque (ft-lb)	1	2	3	4	5	6	8	10

† This table is applicable only for the settings of pot Nos. 5, 6, and 7 at 0.18, 0.12, and 0.40, respectively, and of the strain-gauge amplifier gain at 50.

3. Arm-Transducer Arrangement

The subject's arm was attached to a metallic member that was keyed to the motor shaft, thus acting as a torque transducer. A measure of the torque T_S was provided by a strain gauge mounted on the metallic member. The method of connection between arm and transducer, as shown in Fig. 13, involved a small wrist cast, made for each individual subject,

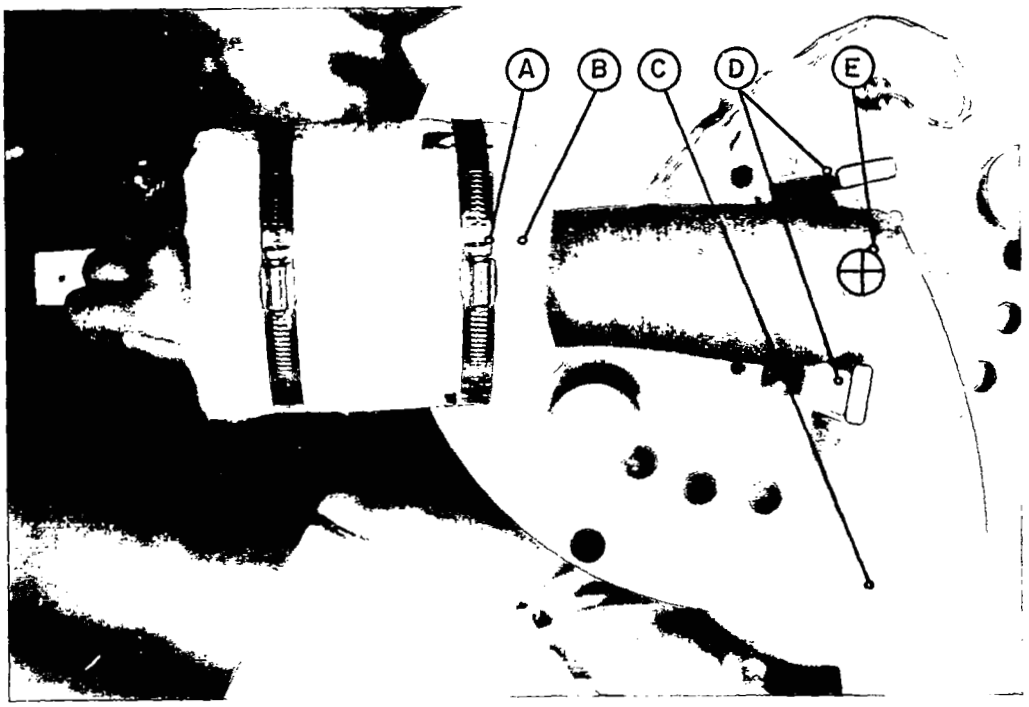

Fig. 13. ARM-TRANSDUCER ARRANGEMENT. Clamp (A) secures the wrist cast (B) to the torque transducer beam. The wrist cast, a polyurethane foam mold of the distal forearm and wrist joint, was prepared for each subject. The mold accurately reflected the contour of the limb and immobilized the wrist joint. The cast can be rotated within clamp (A) to adjust the radio-ulnar joint position. The biceps muscle lies in the frontal aspect of the upper arm (C). Elbow stops (D) locate and restrain the elbow-joint axis (E), holding it coincident with the torque-transducer axis.

that was tightly secured to the transducer by means of a metal clamp. This allowed no play between arm and transducer. Elbow stops located and restrained the elbow-joint axis in a position coinciding with the motor-shaft axis. The seat of the subject (dental chair) always was adjusted so that flexure of the forearm took place in a horizontal plane. This was necessary because implementation of the motor-control system to keep the experiments isotonic was made according to a scalar equation of motion [Eq. (2.13)] for the arm/muscle/electric-motor system; that is, no vector-force component outside of the horizontal plane was considered in the equation of motion. The attachment points of the flexor muscles involved at the shoulder were kept fixed throughout the experiments by strapping the shoulders and chest of the subject securely to the chair.

In the isometric experiments, the transducer or metallic arm is kept fixed by a metal pin through the transducer and the motor platform. In the isotonic experiments, the arm is free and the experiments are initiated with the subject's arm completely relaxed and the motor producing a torque tending to stretch the arm. This torque pushes the subject's arm and the transducer to rest against a stop (plastic peg) that is so positioned that the flexor muscles of the forearm are at their normal resting length (i.e., $\theta = \theta_0 \doteq 40°$).

4. Subject's Safety

Under extreme conditions, the motor is able to develop over 100 ft-lb of torque. This presented a hazard to the subject's safety in the event of a malfunction of the motor or of an error in its operation. For this reason, the angular deflection of the force transducer or metallic arm was constrained by strong mechanical stops (built into the structure of the motor) within the range of forearm flexion that would cause no damage to either the elbow or the shoulder joints. An additional precaution was taken by mounting two microswitches on the transducer, which would open when the metallic arm comes in contact with the mechanical stops and would shut off the motor.

C. Method of Recording Data

All data were recorded on analog magnetic tape, using an Ampex FR 1300 recorder. Six channels were used, and the following time histories were recorded:

(1) forearm angular position, θ

(2) forearm angular velocity, $\dot{\theta}$

(3) forearm angular acceleration, $\ddot{\theta}$

(4) strain-gauge torque, T_S

(5) the stimulus waveform, $a(t)$

(6) the "marker" logic, M

The "marker" logic is a digital subroutine used to label or mark the analog tape for each experimental trial. It consists of a series of pulses whose order of amplitudes provides the key to pertinent information regarding each trial; in particular it denotes

run number

initial forearm angular position

torque applied by electric motor at $\theta = \theta_0 \doteq 40°$

stimulus duration

pulse frequency (stimulus)

pulsewidth (stimulus)

current amplitude (stimulus)

The marker also has the additional function of triggering the digitizing algorithm used in the data analysis that followed the experiments. Unmarked data would be passed over by the digitizing subroutine and would, therefore, not enter the analysis.

It has been noted that a choice of two switches, S and S/M, was available to trigger the stimulus. This is indicated in the experimental

system of Fig. 9. The only differences between these switches are that the S-switch only triggers the stimulator and does not initiate the "marker logic," and the S/M-switch does both. This choice of either "marking" or not marking the tape and not incrementing the run number of the experiment was found desirable because of the great number of unsatisfactory trials at the beginning of an experiment. A great many trials ususlly took place before locating the motor point of the muscle group, determining the amplitude of the stimulus I required for maximal contractions, and obtaining consistency in the muscle torque. Because the data resulting from these preliminary trials were of no interest, no time or effort was devoted to digitizing these data; this was accomplished by using the S-switch, instead of the S/M-switch and, therefore, not marking the tape.

D. Discussion

All the subjects involved in the experiments were normal adults. These experiments were most successful on subjects with slender arms because it was more difficult to locate the motor point and maintain consistent contractions on those with heavier arms.

The sensation felt by the subject as the result of the tetanic and maximal electric stimulation, or shock, is best described as "unpleasant" rather than "painful." Subjects, however, seem to adjust more easily to a maximal contraction, where the stimulating electrode is properly located over the motor point of the muscle group, than to submaximal contractions resulting from the noncoincident muscle-group motor point and electrode. An undesirable sensation resulting from current being propagated subcutaneously to the elbow was observed in the latter case; also, electrodes not located at the muscle-group motor point would occasionally activate other flexors, such as the flexor carpi ulnaris, and these unexpected motor movements were also unpleasant.

Because external stimulation of muscles was totally foreign to all subjects involved in the experiments, some light muscle excitation was performed under low frequencies and amplitudes prior to strapping the subjects to the electric motor/transducer system. This tended to reduce any existing apprehension the subjects might have had about electric

stimulation and to better prepare them for the experiments. Attitude and cooperation were an important part of the experiments because no activation of the muscle group from the central nervous system, voluntary or involuntary, could be tolerated. As a check for possible interference by the central nervous system, or for a slipping or misplaced stimulating electrode, and for any other factor affecting the experimental results, the following precautions were taken.

(1) All trials were repeated until the time histories for strain-gauge torque T_S, in the isometric experiments, and forearm position θ, in the isotonic experiments, would be repeatable (overlapping curves) for at least three consecutive trials.

(2) After all the required data were collected, some of the initial runs were repeated as a "spot check" and compared for consistency. Polaroid photographs of the time histories selected for the spot checks provided immediate comparison.

Most experimental sessions lasted between four and six hours. Although often two or three hours were required before any meaningful data could be recorded, the experiments could not be extended much over five or six hours because fatigue would cause the subject to involuntarily interfere with the data being collected.

Chapter V

EXPERIMENTAL RESULTS

The principal objective of this chapter is to present some of the pertinent data collected from the experiments in their "raw" form. Because neither the process nor the results of mathematical modeling are unique, the experimental results might provide the origin for new paths in seeking a description of the dynamical behavior of human muscle. It is also hoped that the data in the presented form might be of interest to the biologist or physiologist for new and/or different interpretations of the phenomena involved in muscle contraction. All the figures presented in this chapter are reproductions of actual photographs of the raw data, as they appear on an oscilloscope. Before providing sets of compatible data for three individual subjects, a qualitative description of typical results is given.

A. Isotonic Motions

Typical time histories of forearm flexion under isotonic conditions are provided by Figs. 14 and 15; the external loads applied to the

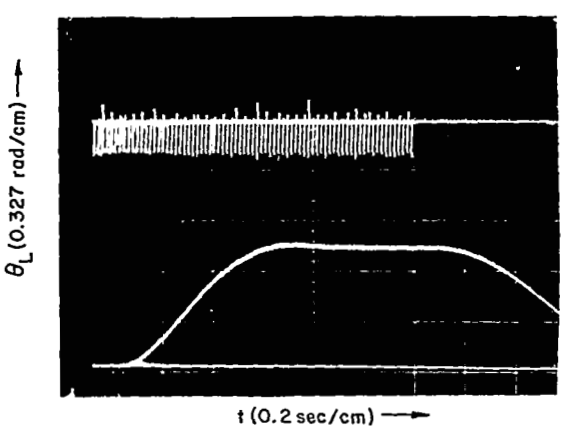

Stimulus { Duration: 1280 ms; Amplitude: 8.0 mA; Frequency: 60/sec; Pulsewidth: 0.5 ms }

Fig. 14. θ_L VS t; T_M = 1 FT-LB AT $\theta = \theta_0$.

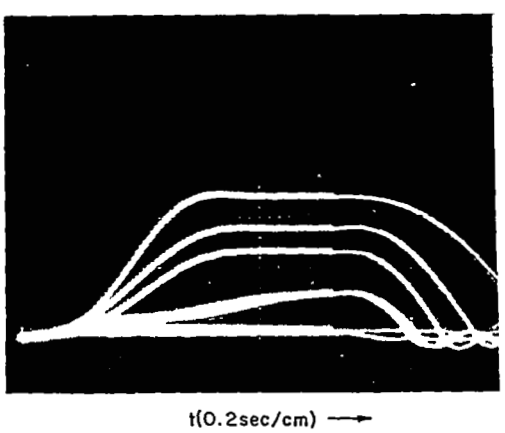

Stimulus { Duration: 1280 ms; Amplitude: 8.0 mA; Frequency: 60/sec; Pulsewidth: 0.5 ms }

Fig. 15. θ_L VS t; T_M = 1,2,3,5,7 FT-LB AT $\theta = \theta_0$.

forearm during the various trials are indicated. It is important to remember, however, that these external loads, applied by the electric motor are functions of both the angular position θ and angular acceleration $\ddot{\theta}$ of the forearm† and that the loads given in the figures apply to the initial conditions of each trial, namely when $\theta = \theta_0$ and $\ddot{\theta} = 0$. Figure 14 also includes the stimulus train of pulses (60/sec) which allows the study of muscle contraction relative to its activation. All traces are triggered by the stimulus, and it is clear from both figures that there is a time delay between the onset of stimulation and the beginning of arm motion. This is not surprising because it was predicted by and accounted for by the mechanism of the postulated model; in fact, this time delay that varies between 100 and 200 ms, depending on the applied load, corresponds to the isometric period discussed in Chapter III and illustrated by Figs. 4 and 5. Some interference of the stimulus with the traces of Fig. 15 can be observed. These traces appear thicker when the stimulus is present and have the helpful, although unplanned, effect of illustrating its duration.

Both Figs. 14 and 15 also indicate a time delay between the end of activation and the beginning of relaxation of the muscles. This delay is about 60 ms. As soon as relaxation begins, the muscle torque can no longer match the applied external load which then brings the forearm back toward its original position until the transducer comes to rest against the mechanical stop. Some bouncing of the arm/transducer system against the stop occurs, as can be observed at the end of the traces of Fig. 15. Indeed, the only data of interest in this investigation are those collected prior to relaxation. Figure 15 shows traces for various loads and indicates that the isometric tension was not high enough to move the largest applied load of 7 ft-lb. Prior to reaching a plateau, some "peaking" of the time histories for the lower loads also can be observed. This implies a higher order highly damped oscillatory motion, however, which is attributed to the dynamic response of the metallic transducer. This effect, therefore, will not be accounted for in the developed model for the muscles.

† Refer to the control logic of Fig. 7 where continuous corrections to the load T_M are made according to the forearm angular position and acceleration.

As discussed earlier, the elements comprising the postulated model are expected to be nonlinear which suggests analysis of the data in the phase plane. Typical phase-plane displays of the data for two different loads are illustrated in Fig. 16. By the definition of "phase plane," these are plots of the coordinate vs its first derivative, namely θ_L vs $\dot{\theta}_L$. Under isotonic conditions $\dot{\theta}_C = \dot{\theta}_L$, and the ordinate can also be labeled $\dot{\theta}_C$ because the purpose of the isotonic experiments is precisely to relate $\dot{\theta}_C$, θ_L, and T_A mathematically to characterize the contractile element, that is, to define explicitly the function $g_2(\cdot)$ of Eq. (2.7),

$$\dot{\theta}_C = g_2(T_A, \theta_L)$$

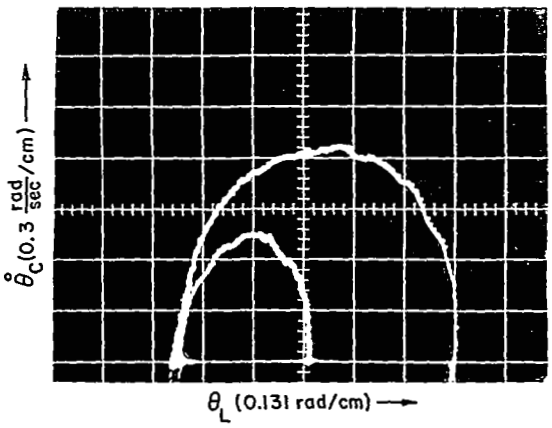

Duration: 1280 ms
Amplitude: 8.0 mA
Frequency: 60/sec
Pulsewidth: 0.5 ms

Fig. 16. $\dot{\theta}_C$ VS θ_L; $T_M = 3,5$ FT-LB AT $\theta = \theta_0$.

It will be shown in the following chapter how phase-plane displays of the data, similar to those of Fig. 16, will form the basis for characterizing the contractile element.

B. Isometric Torque

The information recorded from the set of isometric experiments is typically illustrated by Fig. 17. The data consist of time histories of the developed isometric torque T_A for various angular positions of the forearm θ_L, that is, for various muscle lengths. Because no motion of the arm is involved in these experiments, they are considerably easier to conduct and the results obtained can be amazingly consistent and repeatable. Figure 17 is actually a photograph of four traces resulting from four consecutive trials that were recorded on an oscilloscope in the storage mode, and the traces were triggered by the stimulus. An almost perfect overlap of these time histories can be observed.

The stimulus duration for the trials was 500 ms and, again, it can be observed that the stimulus leads the muscle torque by a short time delay (20 ms); indeed, this delay need not equal the one preceding the start of motion in the isotonic experiments. In the isotonic case, the length of the delay is the time required for the developed muscle torque to equal the applied load and, therefore, depends on the value of the applied load; in the isometric data, the delay preceding the start of muscle-torque buildup is due solely to physiological factors. The delay observed between the end of stimulation and muscle relaxation, however, should be the same in both the isotonic and isometric trials because it depends only on physiological factors. This appears to be the case because, again, the end of the period of stimulation leads the beginning of muscle relaxation by about 60 ms.

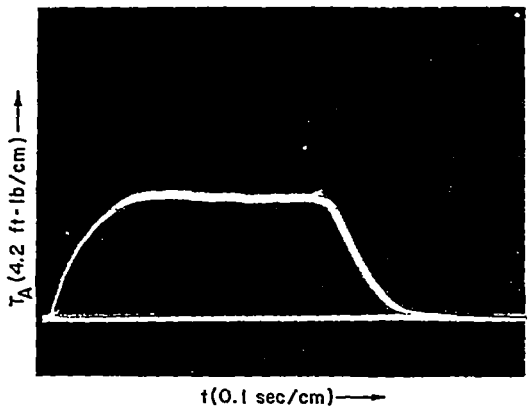

Duration: 500 ms
Amplitude: 8.0 mA
Frequency: 60/sec
Pulsewidth: 0.5 ms

Fig. 17. T_A VS t; $\theta_L = 30°$. (Four repetitions)

For various forearm angular positions, the information obtained from time histories (similar to the one in Fig. 17) permitted θ_L and T_A to be mathematically related and, therefore, characterizes the function $e(\cdot)$ in Eq. (3.5):

$$\theta_L = r(T_A) \tag{3.5}$$

This, in turn, will allow the characterization of the series elastic element, as discussed in Chapter III.

C. Data Sets

This section is devoted entirely to the presentation of some of the original data, as collected directly from the experiments. All the figures are photographs of the raw data displayed on an oscilloscope directly from the analog magnetic tape on which they were recorded.

Compatible data sets for three separate subjects are presented. They are in the form of the data presented in the preceding section, with the addition of some angular velocity $\dot{\theta}_L$ time histories; that is, each set comprises some of the results from both the isotonic and isometric experiments. Figures 18 to 22 present a portion of the data collected on subject 1, Figs. 23 to 27 on subject 2, and Figs. 28 to 30 on subject 3.

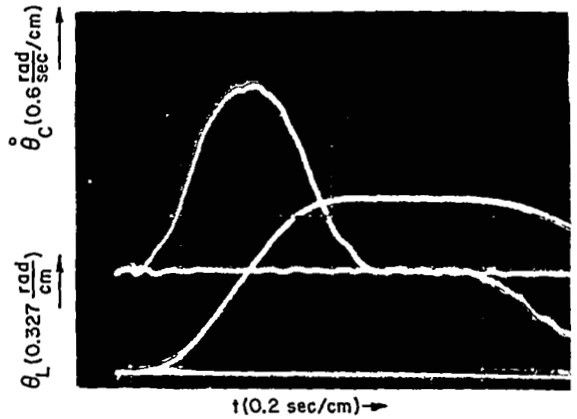

Duration: 1300 ms
Amplitude: 8.0 mA
Frequency: 75
Pulsewidth: 0.8 ms

Fig. 18. $\dot{\theta}_C$ AND θ_L VS t; T_M = 0.1 FT-LB AT $\theta = \theta_0$.

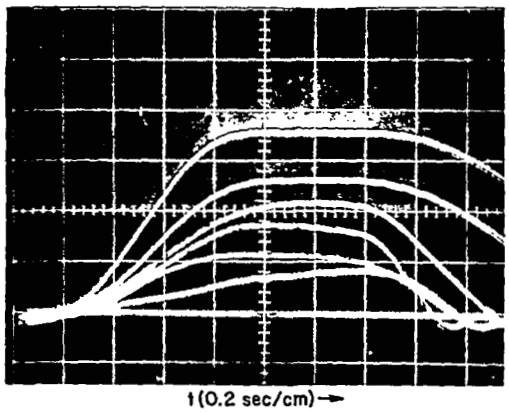

Duration: 1300 ms
Amplitude: 8.0 mA
Frequency: 75
Pulsewidth: 0.8 ms

Fig. 19. θ_L VS t; T_M = 0.1,2, 3,4,5,6 FT-LB AT $\theta = \theta_0$.

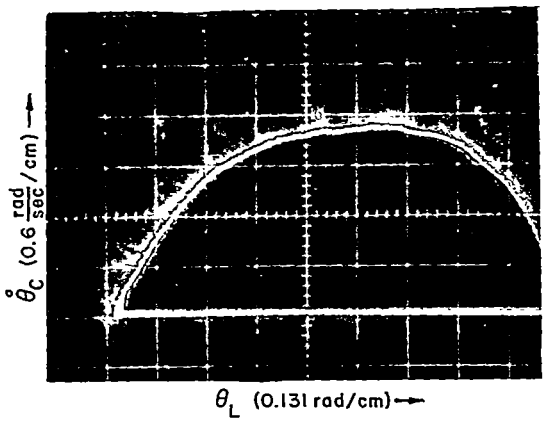

Duration: 1300 ms
Amplitude: 8.0 mA
Frequency: 75
Pulsewidth: 0.8 ms

Fig. 20. $\dot{\theta}_C$ VS θ_L; T_M = 0.1 FT-LB AT $\theta = \theta_0$.

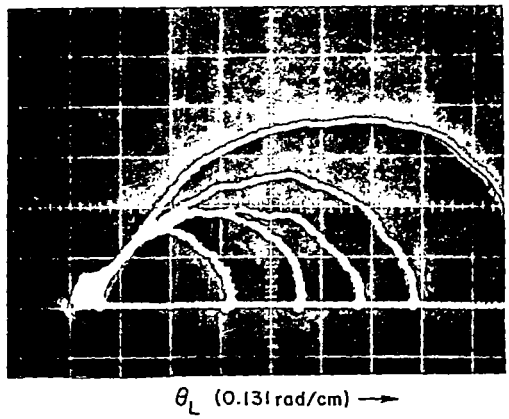

Duration: 1300 ms
Amplitude: 8.0 mA
Frequency: 75
Pulsewidth: 0.8 ms

Fig. 21. $\dot{\theta}_C$ VS θ_L; T_M = 0.1, 2, 4, 5, 6 FT-LB AT $\theta = \theta_0$.

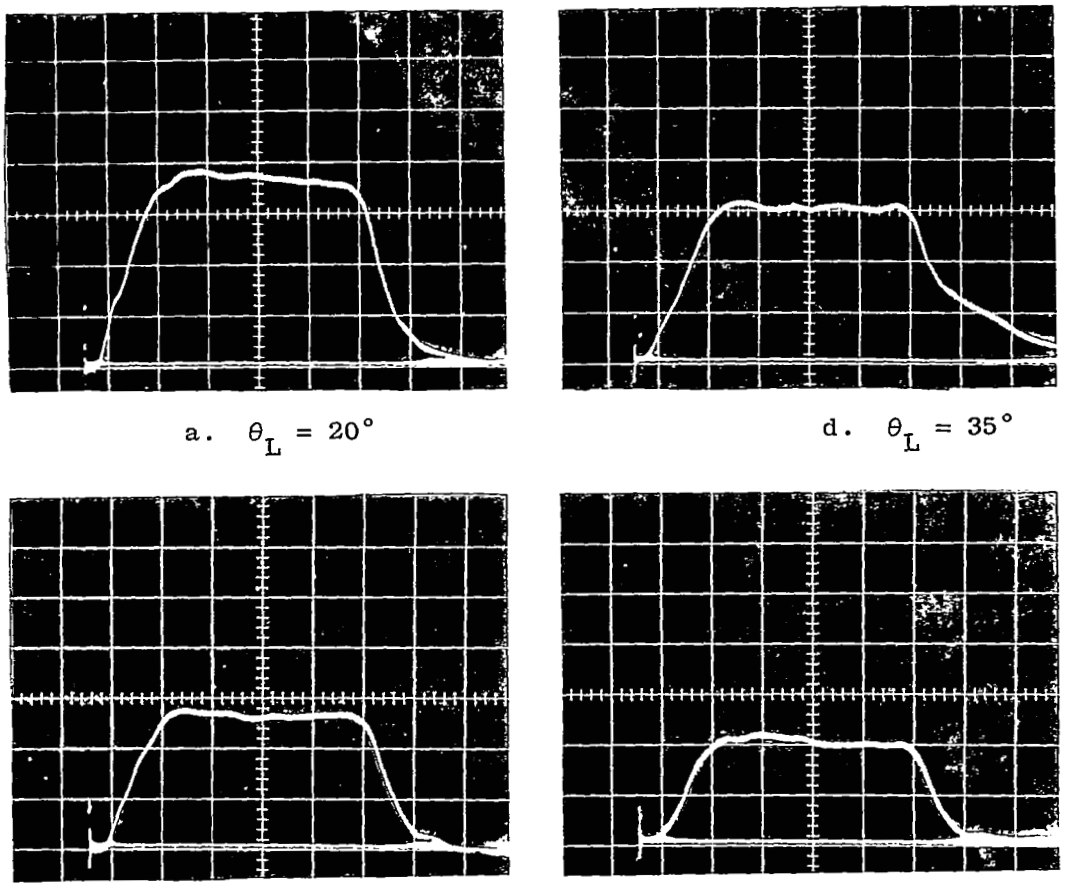

a. $\theta_L = 20°$

d. $\theta_L = 35°$

b. $\theta_L = 50°$

e. $\theta_L = 65°$

c. $\theta_L = 80°$

Duration: 500 ms
Amplitude: 8 mA
Frequency: 75
Pulsewidth: 0.8 ms

Fig. 22. T_A VS t; $\theta_L = 20°$, 35°, 50°, 65°, 80°.

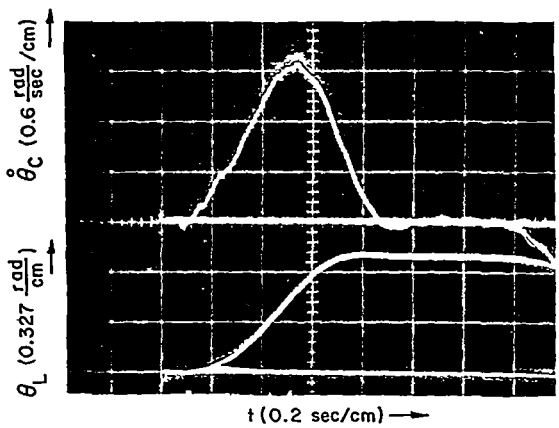

Duration: 1300 ms
Amplitude: 8 mA
Frequency: 60
Pulsewidth: 0.5 ms

Fig. 23. $\dot{\theta}_C$ AND θ_L VS t; T_M = 0.1 FT-LB AT $\theta = \theta_0$.

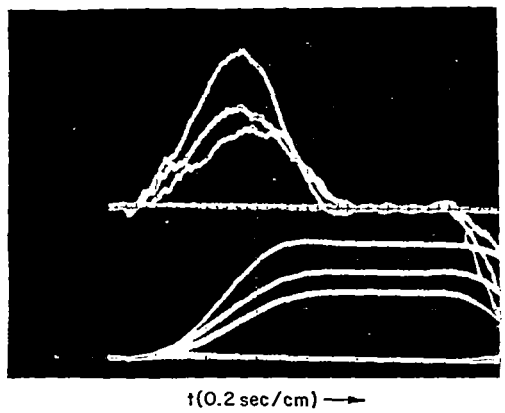

Duration: 1300 ms
Amplitude: 8 mA
Frequency: 60
Pulsewidth: 0.5 ms

Fig. 24. $\dot{\theta}_C$ AND θ_L VS t; T_M = 0.1,2,3 FT-LB AT $\theta = \theta_0$.

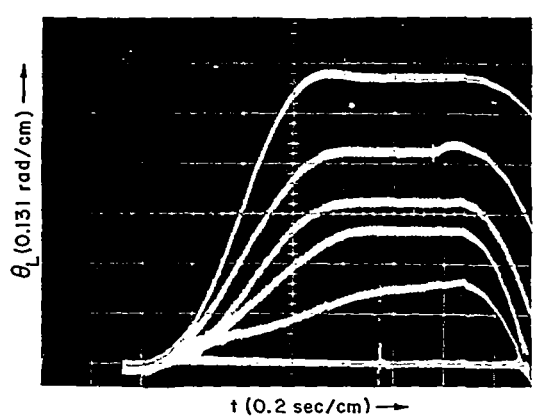

Duration: 1300 ms
Amplitude: 8 mA
Frequency: 60
Pulsewidth: 0.5 ms

Fig. 25. θ_L VS t; T_M = 0.1,2,3, 4,5 FT-LB AT $\theta = \theta_0$.

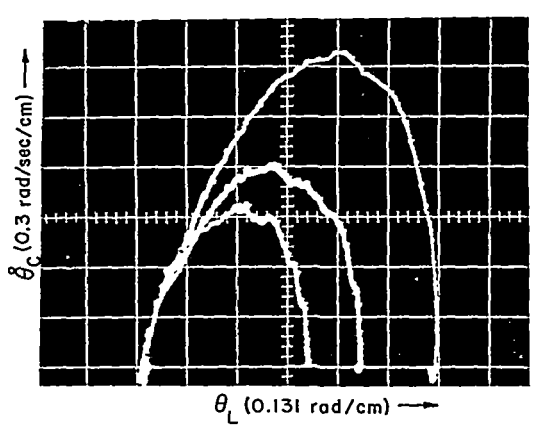

Duration: 1300 ms
Amplitude: 8 mA
Frequency: 60
Pulsewidth: 0.5 ms

Fig. 26. $\dot{\theta}_C$ VS θ_L; T_M = 0.1,2, 3 FT-LB AT $\theta = \theta_0$.

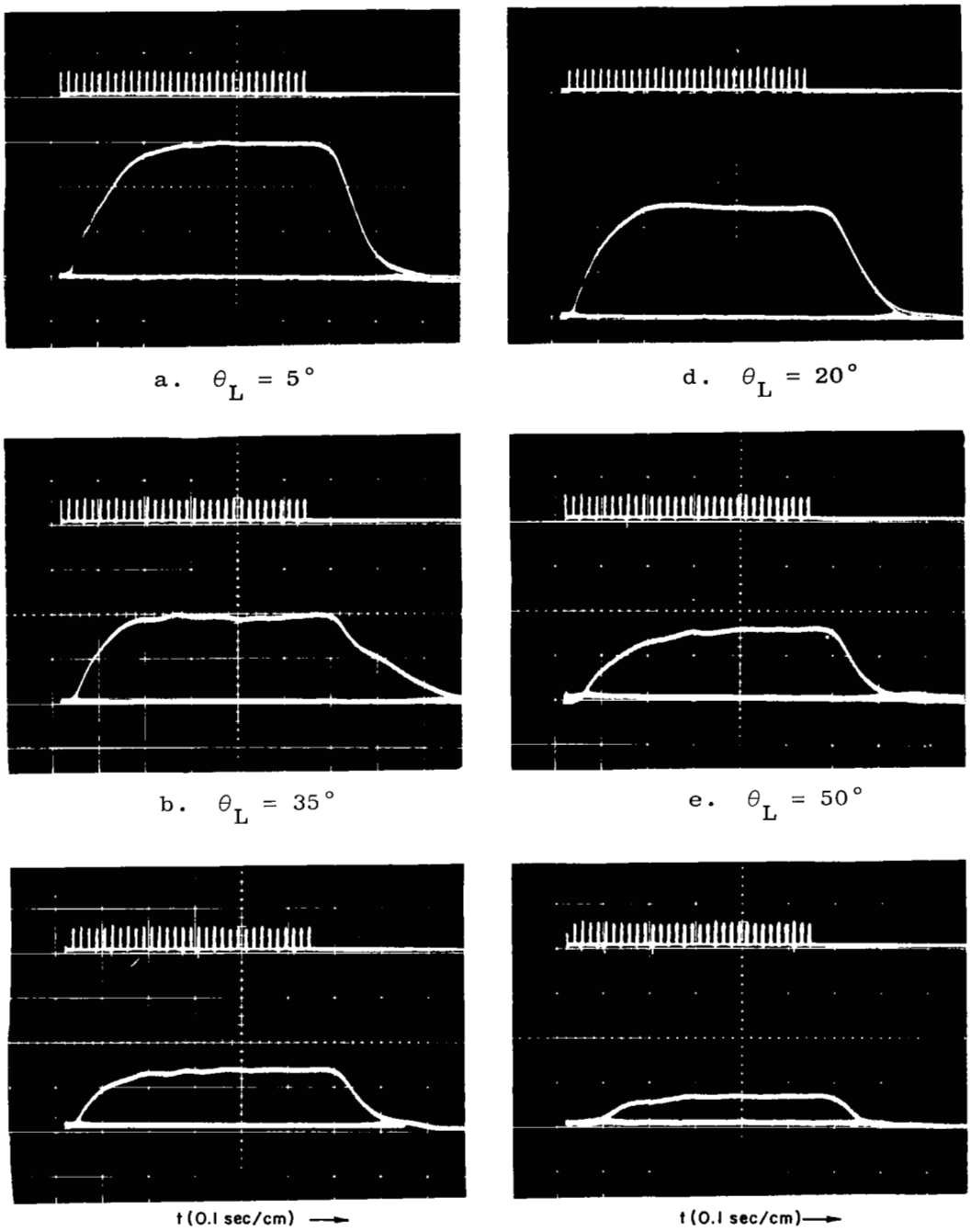

a. $\theta_L = 5°$

d. $\theta_L = 20°$

b. $\theta_L = 35°$

e. $\theta_L = 50°$

c. $\theta_L = 65°$

f. $\theta_L = 80°$

Duration: 500 ms
Amplitude: 8.0 mA

Frequency: 60
Pulsewidth: 0.5 ms

Fig. 27. T_A VS t; $\theta_L = 5°, 20°, 35°, 50°, 65°, 80°$.

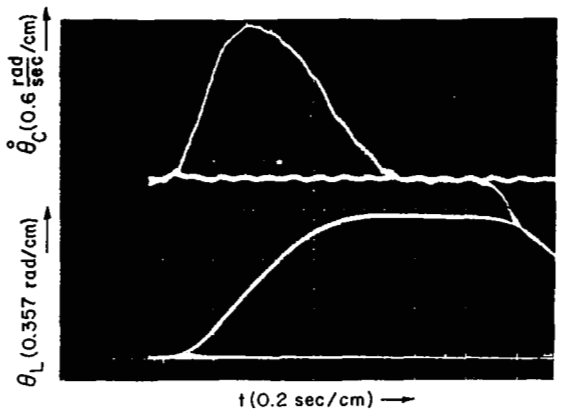

Duration: 1300 ms
Amplitude: 7.5 mA
Frequency: 75
Pulsewidth: 0.8 ms

Fig. 28. $\dot{\theta}_C$ AND θ_L VS t; T_M = 2 FT-LB AT $\theta = \theta_0$.

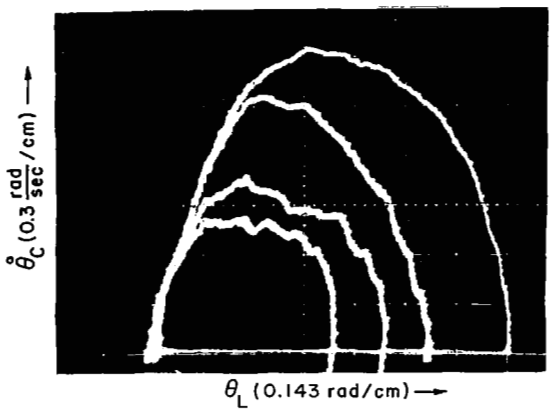

Duration: 1300 ms
Amplitude: 7.5 mA
Frequency: 75
Pulsewidth: 0.8 ms

Fig. 29. $\dot{\theta}_C$ VS θ_L; T_M = 2,3,5, 6 FT-LB AT $\theta = \theta_0$.

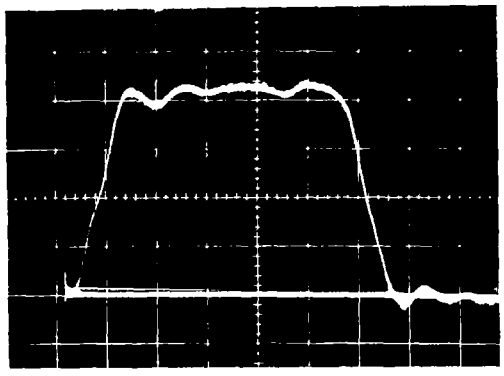

a. $\theta_L = 5°$

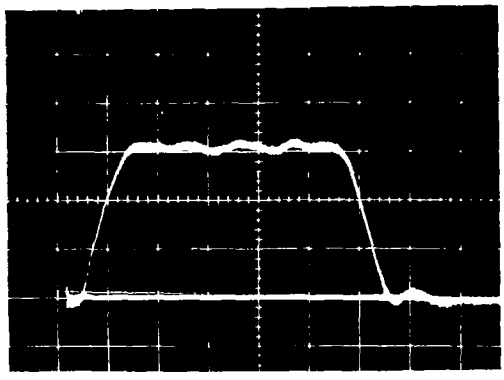

d. $\theta_L = 20°$

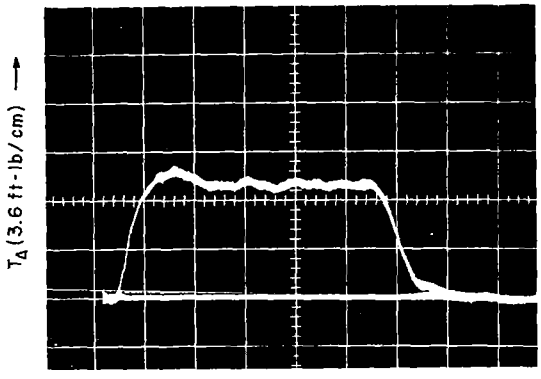

b. $\theta_L = 50°$

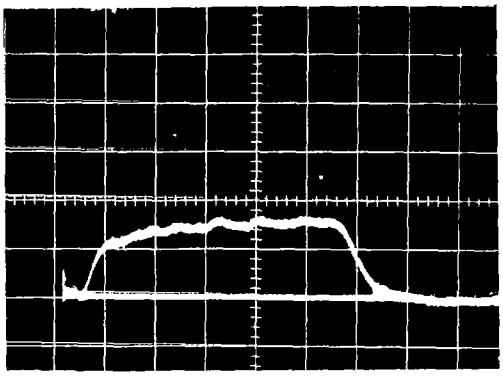

e. $\theta_L = 65°$

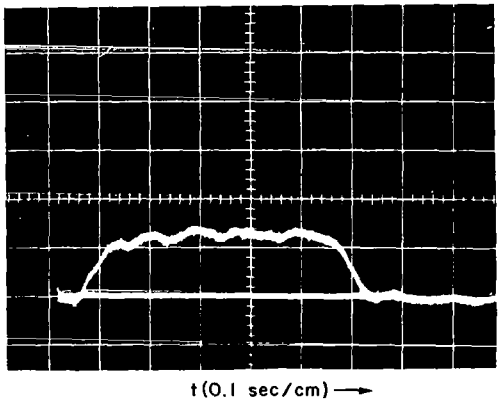

c. $\theta_L = 80°$

Duration: 500 ms
Amplitude: 7.5 mA
Frequency: 75
Pulsewidth: 0.8 ms

Fig. 30. T_A VS t; $\theta_L = 5°$, 20°, 50°, 65°, 80°.

Chapter VI

CHARACTERIZATION OF EQUATIONS FROM EXPERIMENTAL DATA

The chronological steps taken in this investigation and presented in the preceding chapters can be summarized as follows:

(1) postulation of a dynamical mechanism as a model for human skeletal muscle

(2) mathematical description of the model by equations in general forms involving undetermined functions and parameters

(3) formulation of experiments that would permit the identification of the unknown functions and parameters in the equations

(4) experimental procedures and collection of data for the explicit characterization of the undetermined functions and parameters

To obtain a complete mathematical model for the dynamics of the muscles studied, the remaining step is to make use of the data collected to characterize fully the unknown functions $g_1(\cdot)$ and $g_2(\cdot)$ of the model and to determine the parameters comprised by them.

A. The Functions and Parameters Characterizing the Contractile Element

The equation of concern here is

$$\dot{\theta}_C = g_2(T_A, \theta_L) \tag{2.7}$$

and the experiments formulated to characterize the symbolic function were those conducted under isotonic conditions. The approach taken to explicitly describe Eq. (2.7) from the data collected is empirical; the purpose was to determine a general class of curves that would best fit the experimental data. The analog data was digitized on a LINC-8 computer and displayed on an oscilloscope, which provided great flexibility in manipulating the data in the search for curves that would best describe the results. In conjunction with the digital-display approach, the data for

$\dot{\theta}_C$ and θ_L were plotted on linear and semilog and log-log scales. This method, successfully used by Zajac [Ref. 4] to interpret data from cat muscles, did not provide very good results for the forearm flexors. In particular, the functions derived from log-log plots as used by Zajac, although providing great generality, failed to describe the data in the neighborhood of muscular equilibrium where very large decelerations were observed. This rapid change in muscle velocity prior to coming to rest, however, provided the clue to the discovery of a class of curves that were found to best describe the velocity-length function $g_2(T_A, \theta_L)$.

1. General Form of the Velocity-Length Function $g_2(\cdot)$

Display of the data collected from the isotonic experiments into phase-plane plots, as those of Fig. 16, provided the basis for characterizing the velocity-length function. It was observed that the arches of the plots were elliptical; distances from the center of ellipses to their major and minor vertices (a and b, respectively) could be selected, as well as translations of the ellipses along their major axes so as to match the phase-plane plots. Indeed, only the portion of the ellipses that lies in the upper-right quadrant of the coordinate system is of concern.

This development can be better understood by beginning with the general equation for an ellipse, in terms of the familiar coordinates x and y:

$$\frac{x^2}{a^2} + \frac{y^2}{b^2} = 1 \tag{6.1}$$

where a and b are its semimajor and semiminor axes lengths, respectively. If the center of the ellipse is translated a distance T along the abscissa as shown in Fig. 31a, the equation in the upper-half plane becomes

$$y = b\left[1 - \left(\frac{x - T}{a}\right)^2\right]^{1/2} \tag{6.2}$$

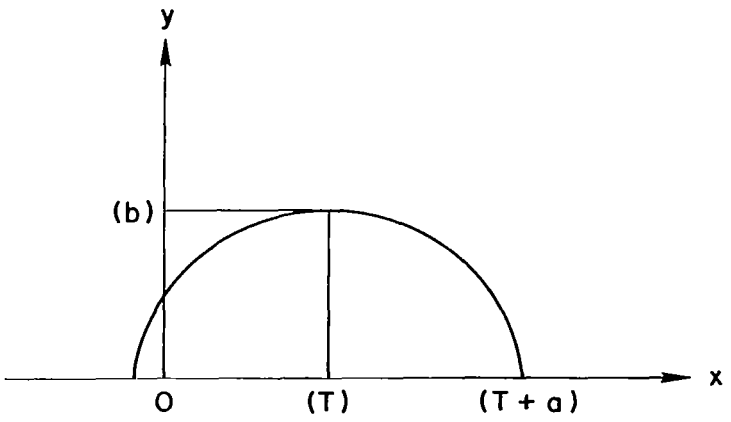

a. $$y = b\left[1 - \left(\frac{x - T}{a}\right)^2\right]^{1/2}$$

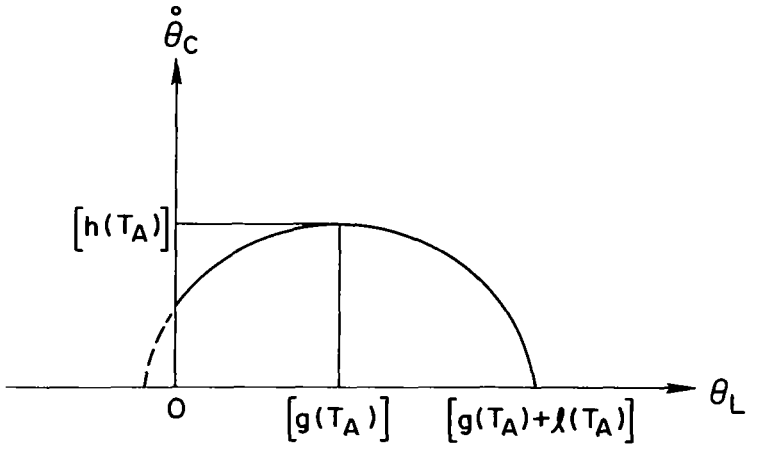

b. $$\dot{\theta}_C = h(T_A)\left\{1 - \left[\frac{\theta_L - g(T_A)}{\ell(T_A)}\right]^2\right\}^{1/2} \qquad \theta_L > 0, \quad \dot{\theta}_C > 0$$

Fig. 31. ELLIPTICAL DESCRIPTION OF ISOTONIC DATA.

Because a, b, and T are selected to have ellipses match the phase planes corresponding to various muscle torques T_A, these parameters

can be expressed as functions of T_A and Eq. (6.2) then can be written as

$$\dot{\theta}_C = h(T_A)\left\{1 - \left[\frac{\theta_L - g(T_A)}{\ell(T_A)}\right]^2\right\}^{1/2} \tag{6.3}$$

where x and y of Eq. (6.1) have been replaced by the coordinates θ_L and $\dot{\theta}_C$, and a, b, T by the functions $\ell(T_A)$, $h(T_A)$, and $g(T_A)$, respectively. The association of these functions with the phase planes is illustrated by Fig. 31b. From Eq. (6.3), the velocity-length function, in turn, can be expressed as

$$g_2(T_A, \theta_L) = h(T_A)\left\{1 - \left[\frac{\theta_L - g(T_A)}{\ell(T_A)}\right]^2\right\}^{1/2} \tag{6.4}$$

The above method of describing the functions $\ell(T_A)$, $h(T_A)$, and $g(T_A)$ would be equivalent to considering a nominal elliptical arch and rescaling it about its major axis according to $\ell(T_A)$ and about its minor axis according to $h(T_A)$ after having shifted the ellipse by $g(T_A)$. This interpretation led to the description of $\ell(T_A)$ as the position-gain function, $h(T_A)$ as the velocity-gain function, and $g(T_A)$ as the translational function. These functions will be characterized explicitly in the following sections.

2. Characterization of the Position-Gain Function $\ell(T_A)$

As discussed previously and indicated on Figs. 4 and 5, the initial portion of the data in all isotonic trials cannot accurately represent the dynamic behavior of the postulated model because the postulated mechanism implies a nonzero velocity of the forearm at the onset of isotonic motion, that is, when motion of the forearm is first observed. For this reason, only the latter parts of the phase-plane curves were used in extracting the data and, when necessary, they were extrapolated back to the initial regions of larger muscular lengths to appear as in Fig. 31b, that is, with $\dot{\theta}_C > 0$ at $\theta_L = 0$.

The position-gain function was derived from the data by tabulating the distances from the center of the extrapolated ellipses (phase planes) to their major vertices (those on the θ_L axis) and the corresponding flexor torque T_A. This information is given in Table 3 for three individual subjects. Curve fitting these data was attempted

Table 3

THE TRANSLATIONAL, POSITION-GAIN, AND VELOCITY-GAIN FUNCTIONS

$$\dot{\theta}_C = g_2(\theta_L, T_A)$$

$$\dot{\theta}_C = h(T_A)\left\{1 - \left[\frac{\theta_L - g(T_A)}{\ell(T_A)}\right]^2\right\}^{1/2}$$

T_A at $\theta = \theta_0$ (ft-lb)	Subject 1			Subject 2			Subject 3		
	$g(T_A)$ (rad)	$\ell(T_A)$ (rad)	$h(T_A)$ (rad/sec)	$g(T_A)$ (rad)	$\ell(T_A)$ (rad)	$h(T_A)$ (rad/sec)	$g(T_A)$ (rad)	$\ell(T_A)$ (rad)	$h(T_A)$ (rad/sec)
0.1	0.524	0.576	2.22	0.366	0.418	1.8	---	---	---
2.0	0.401	0.420	1.50	0.288	0.302	1.2	0.372	0.486	1.86
3.0	0.345	0.399	1.31	0.196	0.236	0.96	0.300	0.472	1.59
4.0	0.305	0.367	1.08	---	---	---	---	---	---
5.0	0.236	0.275	0.94	0.106	0.107	0.64	0.214	0.428	1.11
6.0	0.197	0.199	0.78	---	---	---	0.184	0.310	0.84

by displaying the points on linear semilog and log-log plots. Figure 32 illustrates the linear fit adopted and defined by the parameters of

$$\ell(T_A) = c - nT_A \tag{6.5}$$

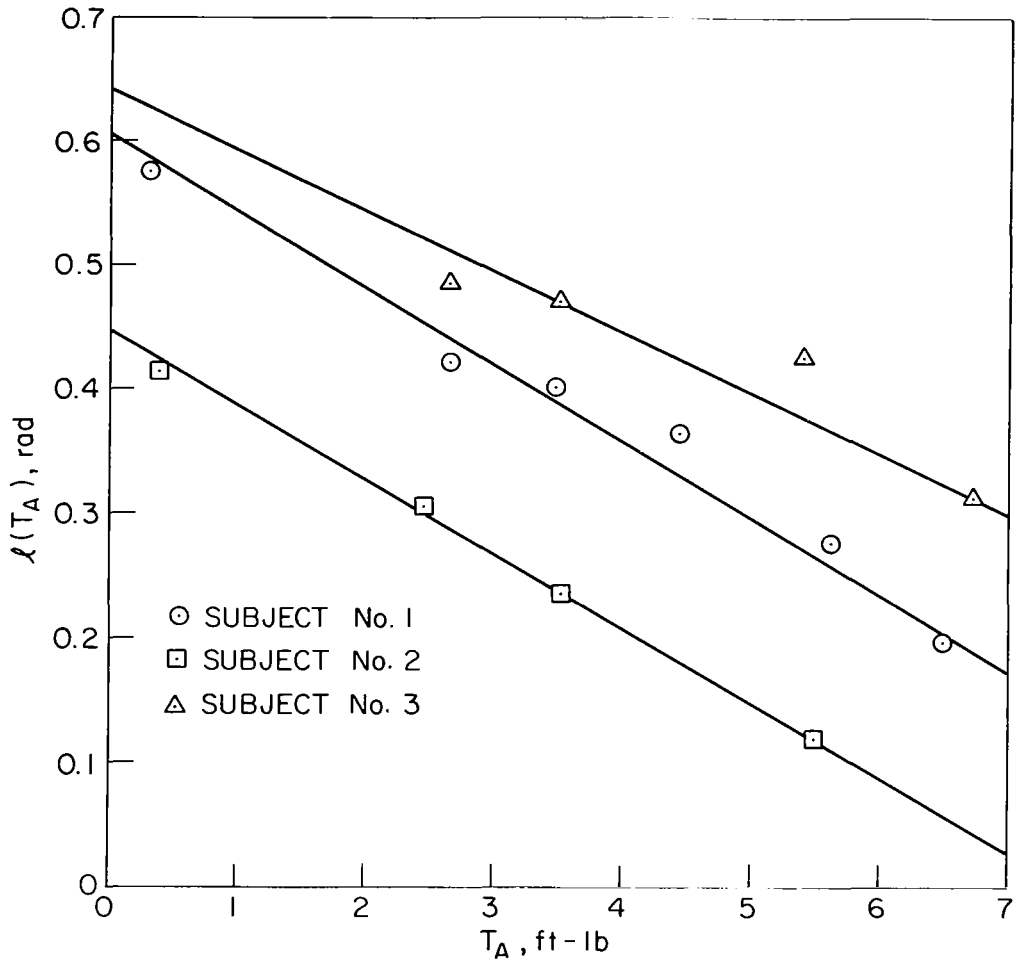

Fig. 32. POSITION-GAIN FUNCTION.

The values for c and n are constants for each individual and are given in Table 4 for five subjects. It is important to note that the values for T_A in Table 3 apply strictly for the flexor muscles at their normal resting lengths, $\theta = \theta_0$; therefore, before plotting, these values must be adjusted according to $1/h_5(\theta_L)$. This is necessary if it is recalled that muscle tension P, and not muscle torque T_A, was maintained constant throughout the arm motions. To account for this, the external load applied to the forearm was controlled to effectively adjust T_A according to the function $1/h_5(\theta_L)$.

Table 4

PARAMETERS FOR THE CONTRACTILE-ELEMENT EQUATION

$$\dot{\theta}_C = g_2(\theta_L, T_A)$$

$$\dot{\theta}_C = U\, e^{-aT_A}\left[1 - \left(\frac{\theta_L + mT_A - b}{c - nT_A}\right)^2\right]^{1/2}$$

Equation Parameters	Subject				
	1	2	3	4	5
U (1/sec)	2.34	1.97	2.88	2.80	2.40
a	0.166	0.210	0.173	0.167	0.214
b	0.550	0.400	0.512	0.510	0.505
c	0.605	0.445	0.640	0.535	0.635
m (1/ft-lb)	0.0531	0.0543	0.0541	0.081	0.0457
h (1/ft-lb)	0.0615	0.0610	0.049	0.0776	0.0740

3. Characterization of the Velocity-Gain Function $h(T_A)$

The procedure here is similar to the one used to characterize the position-gain function. The distances from the center of the ellipses to their minor vertices and the corresponding flexor torque T_A are tabulated for the various trials. In this case, the best fit of the data was obtained by plotting $h(T_A)$ vs the adjusted torque T_A on semilog scales (Fig. 33). The resulting characteristic equation is

$$\log_{10} h(T_A) = -0.434\, aT_A + \log_{10} U \qquad (6.6)$$

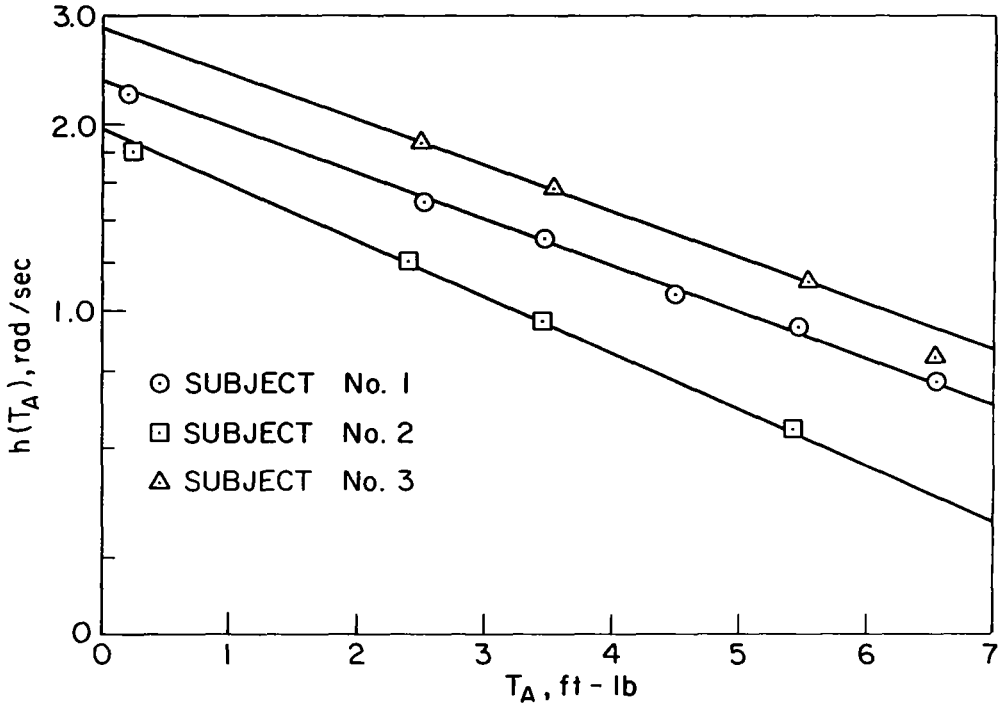

Fig. 33. VELOCITY-GAIN FUNCTION.

or

$$h(T_A) = U\, e^{-aT_A} \tag{6.7}$$

Again, the tabulation of the data and of the resulting parameters are given in Tables 3 and 4, respectively.

4. Characterization of the Translational Function $g(T_A)$

The data of interest in this characterization are the translation of the phase planes along the abscissa for various loads; therefore, the data representing the distances between the center of the ellipses (phase planes) and the origin of the coordinate system were tabulated vs muscular torque in Table 3. A linear fit of these data is shown by Fig. 34 and described by

$$g(T_A) = b - mT_A \tag{6.8}$$

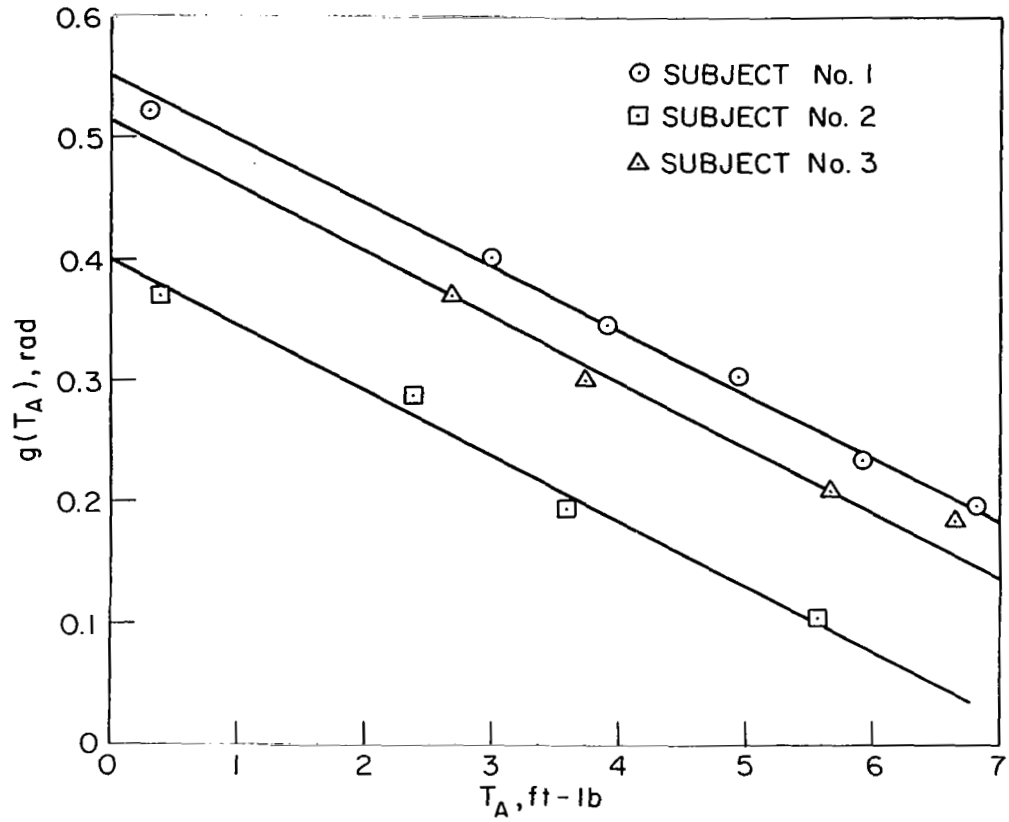

Fig. 34. TRANSLATIONAL FUNCTION.

The values of b and m are given in Table 4 for five individuals.

The results of Section A of this chapter now enable Eq. (2.7) to be explicitly described. In particular, substitution of Eqs. (6.5), (6.7), and (6.8) into Eq. (6.3) yields the complete mathematical model describing the dynamic behavior of the contractile element. The development of this mathematical model comprised a major goal of this research and is given as

$$\dot{\theta}_C = U\, e^{-aT_A} \left[1 - \left(\frac{\theta_L + mT_A - b}{c - nT_A} \right)^2 \right]^{1/2} \qquad (6.9)$$

B. The Functions and Parameters Characterizing the Series Elastic Element

The purpose of this section is to explicitly describe Eq. (2.6) which represents the dynamic behavior of the series elastic element,

$$\theta_C - \theta_L = g_1(P) \tag{2.6}$$

To this end, the results of both the isometric and isotonic experiments will be used in conjunction. Information will be extracted from the isometric data and combined with that obtained from the isotonic data of the preceding sections to characterize Eq. (2.6).

1. The Torque-Length Function $r(T_A)$

The results of the isometric experiments consisted of time histories (illustrated in Chapter V) of developed muscular torque as a function of muscle length or forearm angular position. Table 5 is a tabulation of the maximum torque developed T_A (steady state) for

Table 5

THE TORQUE-LENGTH FUNCTION

$$\theta_L = r(T_A)$$

$\theta_L + \theta_0$ (deg)	θ_L (deg)	θ_L (rad)	T_A (ft-lb)		
			Subject 1	Subject 2	Subject 3
45	5	.0873	---	12.60	13.84
60	20	.3491	14.08	10.48	11.84
75	35	.6109	11.52	8.40	10.44
90	50	.8727	10.08	6.72	9.36
105	65	1.1345	8.28	5.04	6.12
120	80	1.3963	6.12	2.52	5.04

various forearm positions. The approach taken to relate T_A and θ_L mathematically to develop the torque-length function is the same as that used to characterize the position-gain, velocity-gain, and translational functions. Figure 35 indicates a linear fit of the data, giving rise to the following torque-length function for steady-state conditions,

$$\theta_L = r(T_A) = d - kT_A \tag{6.10}$$

The parameters k and d assume constant values for each individual and are given in Table 6.

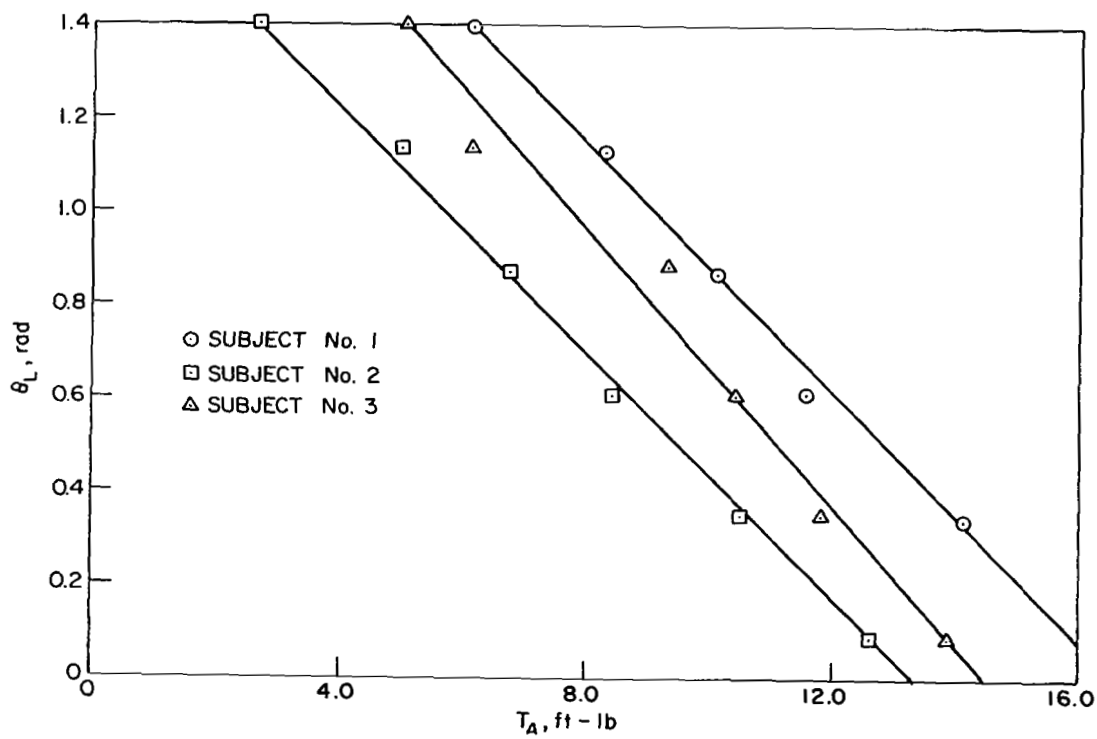

Fig. 35. TORQUE-LENGTH FUNCTION.

Table 6

PARAMETERS FOR THE TORQUE-LENGTH FUNCTION

$$\theta_L = d - kT_A$$

Equation Parameters	Subject		
	1	2	3
k (1/ft-lb)	0.134	0.130	0.147
d	2.21	1.75	2.13

2. Integration of the Velocity-Length Function $g_2(\cdot)$

The mathematical model for the contractile element, as represented by Eq. (6.9), comprises three dependent variables, $\theta_C(t)$, $\theta_L(t)$, and $T_A(t)$. It is not convenient, therefore, to solve this equation by direct integration in its present form; however, by making use of Eq. (6.10), the number of dependent variables can be reduced to two by eliminating either θ_L or T_A. The resulting mathematical model then will lend itself more easily to integration by conventional means. If θ_L is eliminated from Eq. (6.9), the contractile-element velocity can be expressed solely as a function of muscle torque and can be represented as

$$\dot{\theta}_C = g_3(T_A) \tag{6.11}$$

where

$$g_3(T_A) = U\, e^{-aT_A} \left\{ 1 - \left[\frac{T_A(m - k) + d - b}{c - nT_A} \right]^2 \right\}^{1/2} \tag{6.12}$$

subject to the constraint given by (6.10). Integration of (6.11) then yields

$$\theta_C = \int_0^t g_3(T_A)\, dt \tag{6.13}$$

3. Derivation of the Series-Elastic-Element Equation

The description of the series elastic element in symbolic form by Eq. (2.6) now can be represented by a complete and explicit characterization for steady-state torque conditions. This is accomplished by making use of the results developed above, namely, those given by Eqs. (6.13), (6.12), and (6.10). Substituting these results into Eq. (2.6) gives

$$\boxed{\theta_C - \theta_L = \int_0^t g_3(T_A)\, dt - r(T_A)} \tag{6.14}$$

with the constraint

$$\theta_L = d - kT_A \tag{6.10}$$

where $g_3(T_A)$ and $r(T_A)$ were defined by Eqs. (6.12) and (6.10), respectively.

Equation (6.14), therefore, represents the mathematical model for the series elastic element. Combined with Eq. (6.9), it summarizes the results of this study because together they represent the complete characterization of the dynamics of human skeletal muscle sought in this investigation.

C. Relationships between the Functions Characterizing the Contractile and Series Elastic Elements

From the definitions of the translational, position-gain, and torque-length functions, it is important to note the very definite relationship existing between them:

$$g(T_A) + \ell(T_A) = r(T_A) \tag{6.15}$$

This can be observed by referring to Fig. 31b, where the label $g(T_A) + \ell(T_A)$ indicates the forearm position at which equilibrium occurs. At this equilibrium position, the muscle is clearly isometric and the applied load (by electric motor) duplicates the resistance offered by the mechanical device (metal pin) restraining the motion of the metallic arm in the isometric experiments. As a result, the relationship between muscle length (forearm position) and muscle torque $\theta_L = r(T_A)$ in the isometric experiments and $\theta_L = g(T_A) + \ell(T_A)$ when equilibrium is reached in the isotonic experiments must be the same. By making use of Eqs. (6.5), (6.8), and (6.10), the relationship (6.15) can be rewritten as

$$(c - nT_A) + (b - mT_A) = d - kT_A$$

and it follows that

$$b + c = d \tag{6.16}$$

and

$$m + n = k \tag{6.17}$$

Relationships (6.16) and (6.17) provide useful checks for the experimental data and for the numerical values of the parameters entering the mathematical model.

The maximum muscle torque for a given forearm position can be obtained from the constraint equation (6.10) which relates steady-state torque to forearm flexion, as

$$T_{A_{max}} = \frac{d - \theta_L}{k} \tag{6.18}$$

and it now can be observed from Eqs. (6.16), (6.17), and (6.18) that an equivalent constraint equation for maximum muscle force also can be obtained from the results of the isotonic experiments, namely

$$T_{A_{max}} = \frac{(b + c) - \theta_L}{m + n} \tag{6.19}$$

As discussed in the following chapter, these constraints show the dependency of maximum muscle force on muscle length and must be taken into consideration when studying the voluntary control of movement.

D. Summary

1. Model of the Contractile Element

The contractile element was characterized by observing that phase-plane displays of the isotonic data had elliptical shapes; that is, the data could be made to fit ellipses scaled along both their major and minor axes and translated about the abscissa. In particular, the phase planes could be represented by the following elliptical equation:

$$\dot{\theta}_C \simeq h(T_A) \left\{ 1 - \left[\frac{\theta_L - g(T_A)}{\ell(T_A)} \right]^2 \right\}^{1/2} \tag{6.3}$$

The right-hand side of this equation, denoted by $g_2(T_A, \theta_L)$ in the development, is referred to as the velocity-length function. The functions $\ell(T_A)$ and $h(T_A)$ are the scaling variables about the major and minor axes of the ellipses, respectively, and are referred to accordingly as the position-gain and velocity-gain functions. The translational function $g(T_A)$ represents the displacements of the ellipses along the abscissa. The functions $\ell(T_A)$ and $g(T_A)$ were characterized by plotting the data on linear scales, while a semilog scale was used to determine $h(T_A)$. They are represented mathematically as

$$\ell(T_A) = c - nT_A \tag{6.5}$$

$$h(T_A) = U\, e^{-aT_A} \tag{6.7}$$

$$g(T_A) = b - mT_A \tag{6.8}$$

where a, b, c, m, n, and U assume constant values for each individual and are given in Table 4. The final model for the contractile element is

$$\dot{\theta}_C = U e^{-aT_A} \left[1 - \left(\frac{\theta_L + mT_A - b}{c - nT_A} \right)^2 \right]^{1/2} \tag{6.9}$$

2. Model of the Series Elastic Element

The series elastic element was characterized by making use of the model obtained for the contractile element and by extracting the steady-state torque-length function $r(T_A)$ from the data of the isometric experiments. A linear fit of the data described the torque-length function as

$$\theta_L = r(T_A) = d - kT_A \tag{6.10}$$

This relationship permitted the solution of Eq. (6.9) by eliminating θ_L, thus reducing the number of dependent variables in (6.9) to two. The resulting solution for θ_C was represented as

$$\theta_C = \int_0^t g_3(T_A)\, dt \tag{6.13}$$

and the final model for the contractile element was of the following form:

$$\theta_C - \theta_L = \int_0^t g_3(T_A)\, dt - r(T_A) \tag{6.14}$$

subject to the constraint given by Eq. (6.10) where $g_3(T_A)$ and $r(T_A)$ were defined by Eq. (6.12) and (6.10), respectively, and values assumed by the parameters d and k for three individual subjects were provided by Table 6.

The following relationships between parameters identified from the isometric and isotonic experiments were

$$b + c = d \tag{6.16}$$

and

$$m + n = k \tag{6.17}$$

Constraints showing the dependency of maximum muscle force on muscle length are observed from both the isometric and isotonic experiments and given, respectively, by

$$T_{A_{max}} = \frac{d - \theta_L}{k} \tag{6.18}$$

and

$$T_{A_{max}} = \frac{(b + c) - \theta_L}{m + n} \tag{6.19}$$

Chapter VII

DISCUSSION

This chapter discusses several factors bearing on the experimental procedures, the significance of the results, the accuracy of the model relative to the experimental data, a comparison of the results with related work by previous investigators, and the theory guiding the experimental methods. Some speculation about the sensory processes involved in the control of force and position is made on the basis of the results of this study. It is pointed out also how a similar investigation involving asynchronous and nonmaximal stimulation could clarify some of the questions regarding the existence of separable populations of tonic and phasic neuromuscular systems [Ref. 6]. Experiments conducted under such stimulation would have more direct applications in the development of bioelectric prosthesis and the artificial stimulation of muscles to replace efferent signals for paralyzed patients, due to an upper motor lesion, whose muscles are in a normal state.

A. Electromyograms

When any muscle fiber is stimulated, the depolarization of its membrane produces an electric field whose potential appears across any pair of electrodes in the vicinity. The electromyogram (EMG) is the combined effects of the fields of all muscle fibers in a muscle, as observed with a pair of electrodes not inside a muscle fiber. Although the electrical membrane potential is fairly well defined, the EMG signal seen in any voluntary contraction is the interaction of the potentials created by a great many muscle fibers being excited in some random manner. The electrical properties of the tissue surrounding the muscle and the geometry of the various fibers relative to the electrodes are major and complex factors that affect the EMG signals and contribute to rendering its characteristics rather obscure. Although not having a well-defined behavior, however, the EMG signals do provide a measure of motor nerve excitation, at least in average amplitude. It was hoped while formulating the experiments, that EMG activity for both the flexors and tensors of the forearm could be monitored throughout the experiments. The information provided

by the EMG signals would not enter directly into the formulation of the models developed, but they would guide the experiments by

(1) ensuring that the applied excitation is effective and indicating an improper location of the stimulating electrode on the flexor muscles (sliding electrode or relocation of motor point); in addition to not providing the desired constant stimuli to the agonist, the latter might also result in unwanted antagonist activation

(2) indicating subject's interference through voluntary or involuntary reflex activation of the agonist and/or antagonist and unwanted excitations of any source that would invalidate the data

Considerable effort and time, therefore, were devoted to recording external EMG over the muscles active about the elbow. Various geometrical relationships between the locations of the EMG electrodes and the stimulating and ground electrodes were attempted in an effort to minimize the EMG signal disturbance by the stimulating waveforms. In all cases, the waveform effects, unfortunately, could not be suppressed enough for meaningful observations. The signal recorded from the electrodes never seemed to be a pure superposition of a normal EMG activity with the stimulating train of pulses. The current flow between the stimulating and EMG electrodes appeared to have irregular resistances that rendered the interpretation of the recorded signal too complex to be valuable for the above guidelines.

As mentioned above, however, records of EMG activity were not an essential part of the experimental methods. It is believed that the increased repetitions for each experimental trial, the "spot check" procedure (described in Chapter IV) and, perhaps, the additional care exercised in running the experiments provided a substitute for the information that had been expected from EMGs. It also became obvious that the identical time histories (overlapping traces on the oscilloscope display) obtained for consecutively repeated trials would not and did not occur when a change in the location of the stimulating electrode occurred or when excitations other than the controlled ones were present. It became apparent also that any excitation of the antagonist was detected

easily by the resulting disturbance in the "plateau" of both the muscle-torque and forearm-flexion time histories.

The recording of EMG is considerably more important when the data collected are random in character, as in the case of muscle-fiber and neuronal-activity firing rate and action-potential amplitude under voluntary contractions, which potentially lead to both estimation and identification problems. The experimental conditions and techniques used in this investigation, however, provided data that suggested a purely deterministic identification problem where the functions and parameters representing the plant or model were to be obtained. This deterministic nature of muscle dynamics was pointed out by Ritchie and Wilkie [Ref. 7] during their discussion of muscular contraction:

> "... we are not dealing with random errors, for a given muscle consistently gives a force-velocity curve of the same shape."

B. Evaluation of Model

The model developed from the results of the isotonic experiments, which constitutes the basis for the descriptions of both the contractile and series elastic elements, is evaluated in this section. Phase-plane plots computed from the derived model, Eq. (6.9), are compared with actual collected data, and the results are illustrated in Fig. 36 where the evaluation is made for three values of muscle force. Such a comparison is not as straightforward as it appears because, again, the change in geometry of the arm/muscle system complicates the evaluation. It must be remembered that the data comprising the phase-plane plots as displayed are for constant muscle force and not for constant muscle torque. Accordingly, adjustments in the value of muscle torque must be made for each corresponding forearm position when computing phase planes from the model.

As expected, the model predicts faster contractions of the contractile element at the onsets of forearm motions than the actual observed muscular contractions. This is compatible with the model postulated for the muscle as a whole and was discussed in Chapter III. Namely, under real physical conditions, the velocity of the observed muscular contraction cannot instantaneously match the nonzero velocity of the contractile

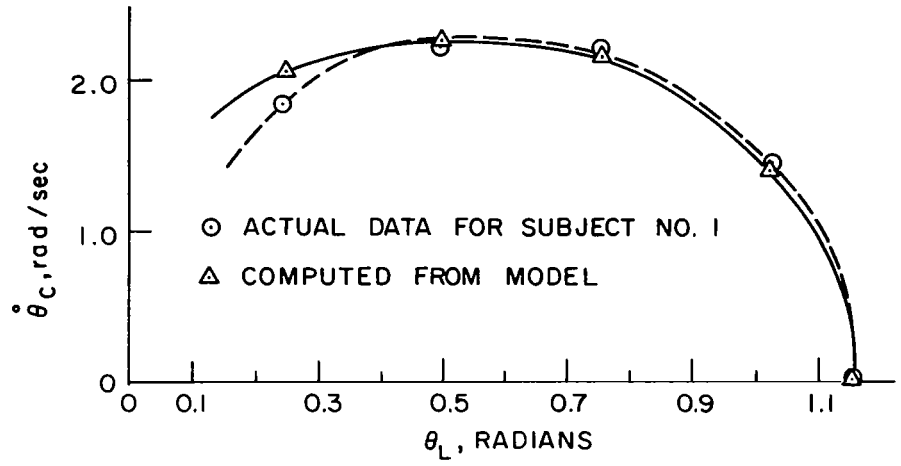

a. T_A = 0.1 ft-lb @ $\theta = \theta_0$ or $\theta_L = 0$

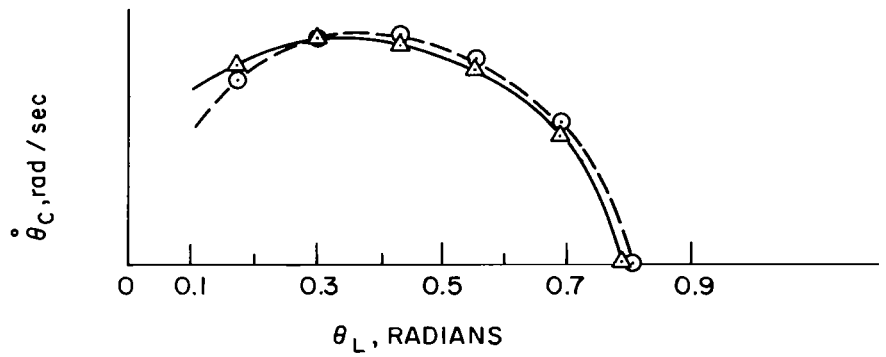

b. T_A = 2.0 ft-lb @ $\theta = \theta_0$

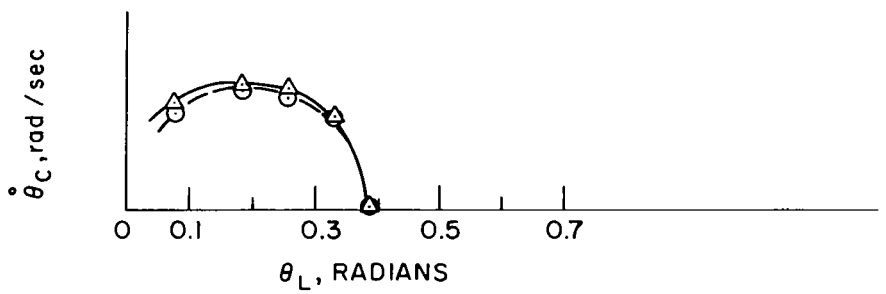

c. T_A = 6.0 ft-lb @ $\theta = \theta_0$

Fig. 36. COMPARISON OF CONSTANT-FORCE THEORETICAL AND EXPERIMENTAL CURVES.

element at the onset of motion, as predicted by the model. A small time delay is required for these velocities to meet the theoretical prediction of their equality under isotonic conditions.

C. Comparison of Model

The best known mathematical description of muscle behavior was derived by Hill [Ref. 1] and given by

$$(P + \alpha)(V + \beta) = \beta(P_o + \alpha) \tag{7.1}$$

where

P = external force

V = shortening velocity of the muscle

P_o = maximum isometric tension

α, β = constants

The principal limitation of this model is that it does not account for the length of the muscle, which was subsequently found to be a definite factor influencing the velocity and the tension in muscles [Refs. 8, 9, 10, and 4]. Hill's equation, therefore, relates muscle force and shortening velocity only at the studied muscular length which was the "normal resting length." This is the most notable distinction between Hill's model and the model developed in this investigation, Eq. (6.9), where the contractile-element velocity is explicitly described as a function of both muscle force and length.

Although Hill's experiments were conducted on the frog's sartorius muscle in vitro at 0°C, it is interesting to compare our results for human muscle in situ with his model. This is done in Fig. 37, where the contractile element's shortening velocity is plotted vs muscle force at "normal resting length." The transformations in Appendix A were used to convert angular velocity and torque to translational velocity and force, respectively. The main difference is in the nonlinearity of those curves; Hill's have a more pronounced curvature. They both display a similar decaying shape for the velocities involved, however, with the exception

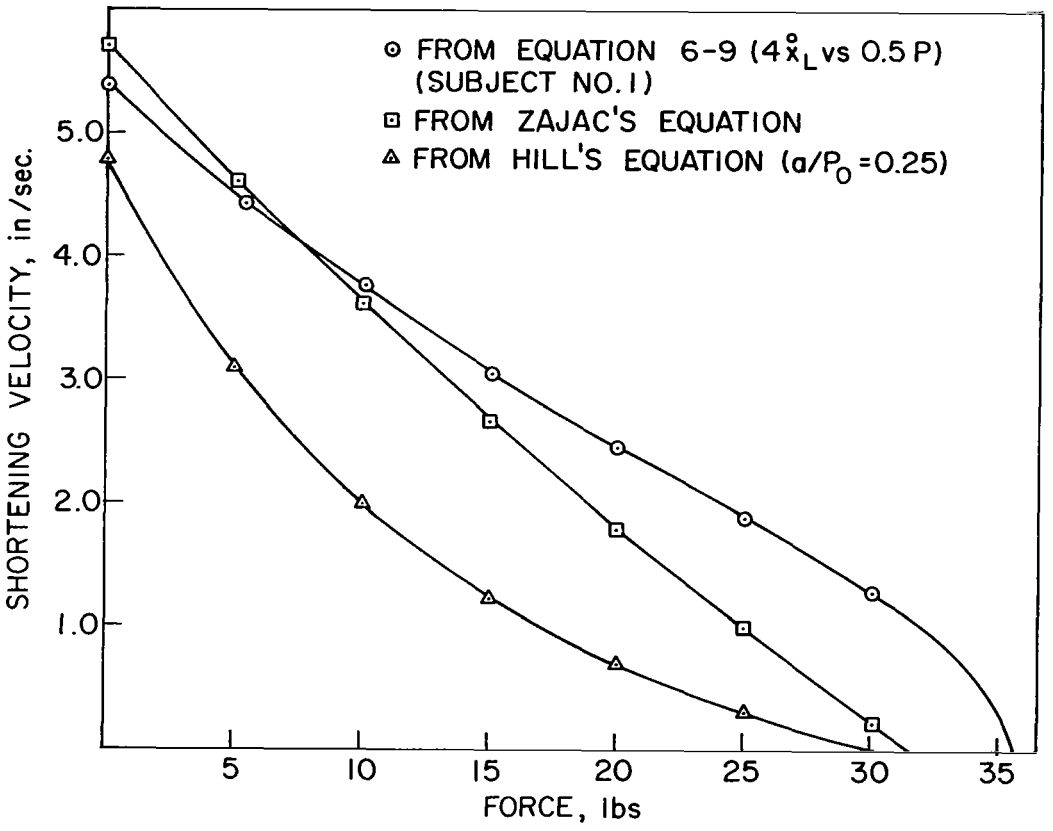

Fig. 37. VELOCITY-FORCE CURVES FOR CONTRACTILE ELEMENTS AT NORMAL RESTING LENGTHS.

of the region close to equilibrium which is attributed to the very large changes in velocities observed in our data near the equilibrium region (see Chapter V). Differences are expected in these results on the basis of the differences in experimental conditions (in vitro vs in situ) and on the fact that Hill performed his experiment on frog muscles and not on human skeletal muscle. The long-discovered discrepancies between model predictions and actual data collected for frog muscles under similar environmental conditions have motivated many investigators to re-examine the theoretical results for muscle behavior. Jewell and Wilkie [Ref. 11] tested the model extensively and reported a "clear" discrepancy between the theoretical prediction and their experimentally obtained velocity-force curve. Carlson [Ref. 12] also showed that Hill's equation could not describe his data at the longer muscular lengths.

Fenn and Marsh [Ref. 13] and more recently Zajac [Ref. 4] studied the shortening characteristics of cat muscle. Zajac, in particular, used isotonic shortening data to model the kinematic properties of the cat's medial gastrocnemius muscle in vivo. His development was not restricted to one specific muscle length but elegantly reflected the dependence of the contractile-element velocity on both muscle force and length. His results are given by

$$\dot{x}_C = V_o \exp(-P/a_v)\left[\left(\frac{|L_o - x_L + k_x P|}{L_o - L_S}\right)^c - 1\right] \tag{7.2}$$

where

$\dot{x}_C$ = contractile-element velocity

x_L = muscle length

P = muscle force

and the other parameters are constants, for a given muscle, obtained empirically from his experimental data. A great deal of similarity can be observed between Zajac's model and the one derived in this investigation. The notable differences, however, are the following.

(1) The shape of the velocity-length curves for a constant force are defined by the power constant c for each muscle, where c is the slope obtained empirically by plotting velocity vs length on log-log scales. Such a description provides great generality and can closely match the elliptical shapes characterized in our model, excluding the region near equilibrium.

(2) If the concept of a velocity-length curve for a nominal force is considered, which is rescaled and translated so as to describe the data for forces other than the nominal, then it is observed that no scaling along the muscle-length axis is implied in Zajac's model.

These differences are illustrated in the following general representations:

$$\dot{\theta}_C = h_T(T_A) \cdot f_T\left[\theta_L \ell_T(T_A) - g_T(T_A)\right] \tag{7.3}$$

$$\dot{x}_C = h_P(P) \cdot f_P\left[x_L - g_P(P)\right] \tag{7.4}$$

where (7.3) represents the model obtained in this study, and (7.2) is the model obtained by Zajac for cat muscle. Difference (1) is the dissimilarity in the functions $f_T(\cdot)$ and $f_P(\cdot)$, where the former is an elliptical function and the latter is described by the power constant c. Difference (2) appears as the lack of a counterpart for the position-gain or scaling function $\ell_T(T_A)$ in Zajac's equation. This has the surprising implication that all the velocity-length curves obtained for cat muscle under different loads have identical shapes near the equilibrium length, and is illustrated by Fig. 38, where the curves for the larger forces are translated to shorter muscle lengths to indicate the identical shapes (overlapping curves) that they would have in the neighborhood of equilibrium. This was not the case for our experiments on human muscles.

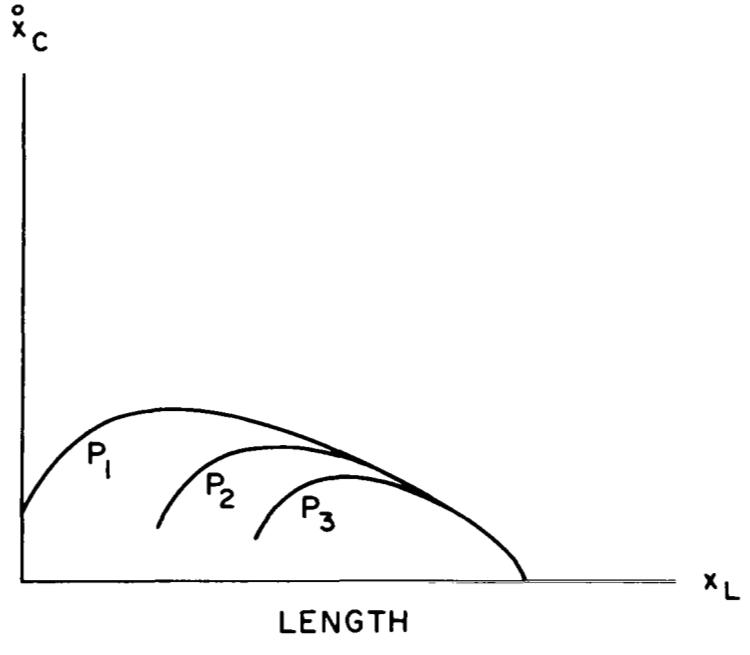

Fig. 38. OVERLAPPING PHASE-PLANE PLOTS FOR DIFFERENT LOADS NEAR MUSCLE EQUILIBRIUM LENGTH, AS IMPLIED BY ZAJAC'S EQUATION. $P_3 > P_2 > P_1$. x_L = distance shortened. Curves for P_2 and P_3 translated to shorter muscle length.

The velocity-force curve for Zajac's equation is also included in Fig. 37 for comparison with our results and Hill's; its shape resembles the velocity-force curve derived from this investigation except in the neighborhood of the equilibrium position, as anticipated. It is also observed from these curves that, although significantly larger loads could be moved by human muscles, the shortening velocities of frog and cat muscles are two to four times faster.

An angular velocity-muscle torque plot at normal resting length is presented in Fig. 39 for completeness; also included is a maximum velocity-torque curve, given by

$$V_{max} = h(T_A) = Ue^{-aT_A} \tag{7.5}$$

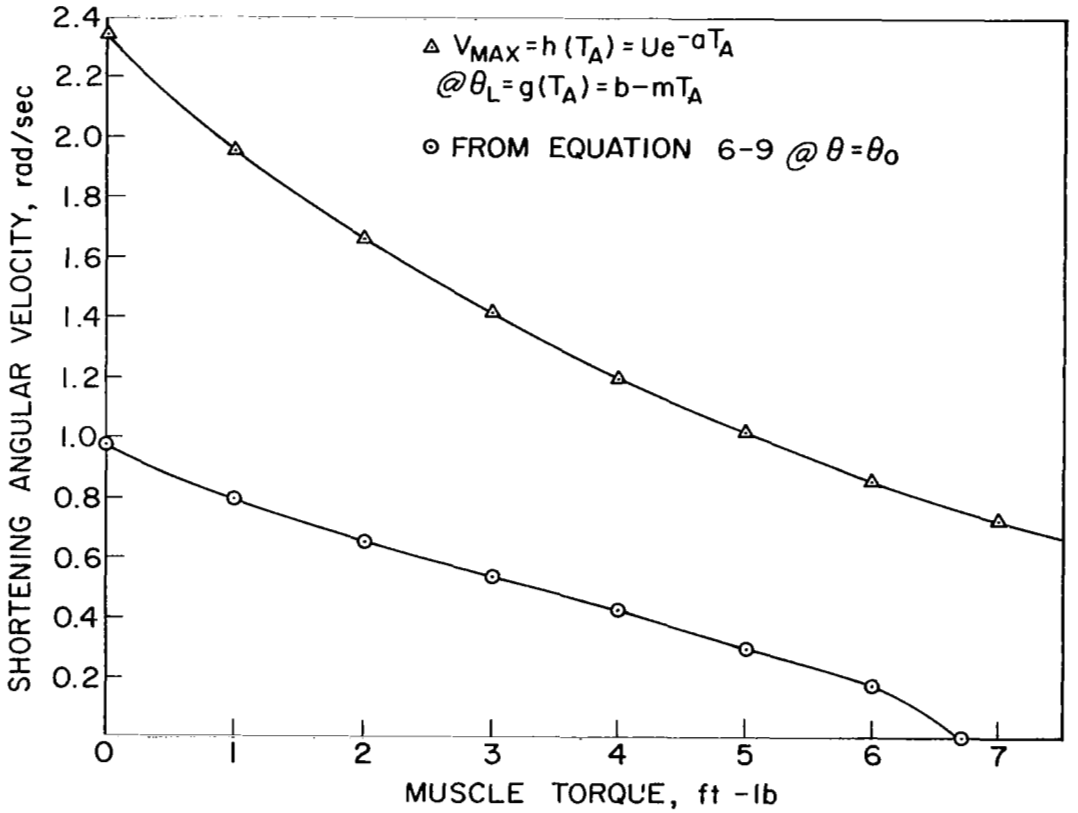

Fig. 39. ANGULAR-VELOCITY VS TORQUE CURVES FOR CONTRACTILE ELEMENT. Subject 1.

with the observation that the maximum shortening velocity occurs at different muscle lengths for different loads. The muscular lengths at which maximum velocity occurs are

$$\theta_L\Big|_{V_{max}} = g(T_A) = b - mT_A \tag{7.6}$$

D. The Control of Movement

This section is concerned with an old problem of considerable interest to both psychologists and neurophysiologists and can be stated by the following question: When impulses leave the motor cortex via the axons of corticospinal neurons, do they specify muscle tension or muscle length?

Numerous studies have been conducted, with varied approaches, in an attempt to discover whether the primary parameter of motor output is force or position. The neurophysiologist has been able to observe patterns of discharge of corticospinal neurons but has been unable to relate these patterns to voluntary movement; whereas, the psychologist has studied normal movement but without hope of knowing the patterns of neuronal discharge correlative with this movement. Unfortunately, because of the complexity of the system, most conclusions have been tentative, with a certain amount of speculation and bias. The hypothesis in this section for the control of movement is no exception and is not immune to the above weaknesses. In any case, the results of investigations devoted to this problem must be interpreted with caution. For example, in discussing his experimental results illustrating a formal relationship between pyramidal tract neurons (PTN) activity and force, Evarts [Ref. 14] warns that a different type of experiment and analysis might have shown an equally convincing relationship between PTN activity and displacement.

When pertaining to the voluntary control of movement, conclusions derived from the results of experiments involving electrical stimulation must be adopted with reservation because most stimulations were conducted maximally and at tetanic frequencies and conclusions drawn from these restricted cases have often been extended to encompass other modes of

stimulation and the voluntary control of movement. In his discussion of the voluntary control of movement, Zajac [Ref. 4] emphasizes the dependence of force not only on excitation but also on muscular length. This is indeed true for maximally and tetanically stimulated muscle (i.e., for maximum force), as illustrated from the isotonic and isometric experiments in this investigation; for different loads, the forearm comes to rest at different positions, and different maximum isometric forces are developed at different muscular lengths. This cannot apply to voluntary control, however, where it is obvious from daily experiences that the same force (within limits discussed below) can be exerted at different limb positions. Partridge [Ref. 15] observed the same amount of contractions for constant but nontetanic stimulations although the muscle was subjected to different loads; this indicates different forces at the same muscle length which suggests that, at least for his mode of stimulation, force is not dependent on muscle length.

The foundation of the hypothesis discussed below is based on the observations of Partridge and Leifer and is guided by the results of this investigation. Partridge noted that, for a given waveform frequency, the muscle will shorten to the same length regardless of the load; more recently, Leifer observed little variation in the neuronal discharge of muscle fibers held at a fixed length. These results could imply that the neuromuscular-unit firing rate, or frequency of stimulation, may specify muscle length. Leifer also observed that the recruitment of additional neuromuscular units was directly proportional to the developed isometric force accounting for 85 to 90 percent of force modulation, thus indicating that the amplitude of stimulation is mainly responsible for developed force. These results suggest, therefore, independent functions for the excitation frequency and amplitude, namely the control of position and force, respectively; furthermore, the results of this investigation indicate definite constraints on the maximum force developed in the muscle. Maximum force is produced under maximal and tetanic neural excitation and its upper limit is dependent on muscle length. The constraint, in rotational form, derived from the isometric experiments is given by

$$T_{A_{max}} = \frac{1}{k} (d - \theta_L) \tag{6.18}$$

or, when derived from the results of the isotonic experiments, by the equivalent equation:

$$T_{A_{max}} = \frac{(b + c) - \theta_L}{m + n} \tag{6.19}$$

Figure 40 is a block diagram of such a hypothesis for the voluntary control of movement, where the amplitude and frequency of neuromuscular excitation are considered to control muscle force and position, respectively, with the above given constraints. This representation is only complete for the agonist; a totally analogous system for the antagonist is implied.

The main feedback logic assumed in this mode of operation is the control of force based on the internal sensing of position or muscle length. As a simple description of this system, consider two motions under identical external loads with the motor commands from the higher centers having the same frequency and different amplitudes. According to the above hypothesis, this would imply identical position commands, but the different amplitudes imply different muscle forces in the open-loop system. According to our control logic, these differences in force would be manifested by different velocities in the movements and, therefore, different durations of the movements because velocity is the single integral of force, and displacement is its double integral, as indicated in Fig. 40. Because the final limb position must be the same (identical frequencies) and the external load applied to the muscles are also the same in both cases, the final muscle force must also be identical when the commanded equilibrium position is reached. Such regulation of the force during movement is achieved by the intrinsic servomechanism involving continuous sensing of position, or its comparison with the desired one. This is shown in Fig. 40, where the transformation of the position sensor signal to the compensating command is denoted by "block K."

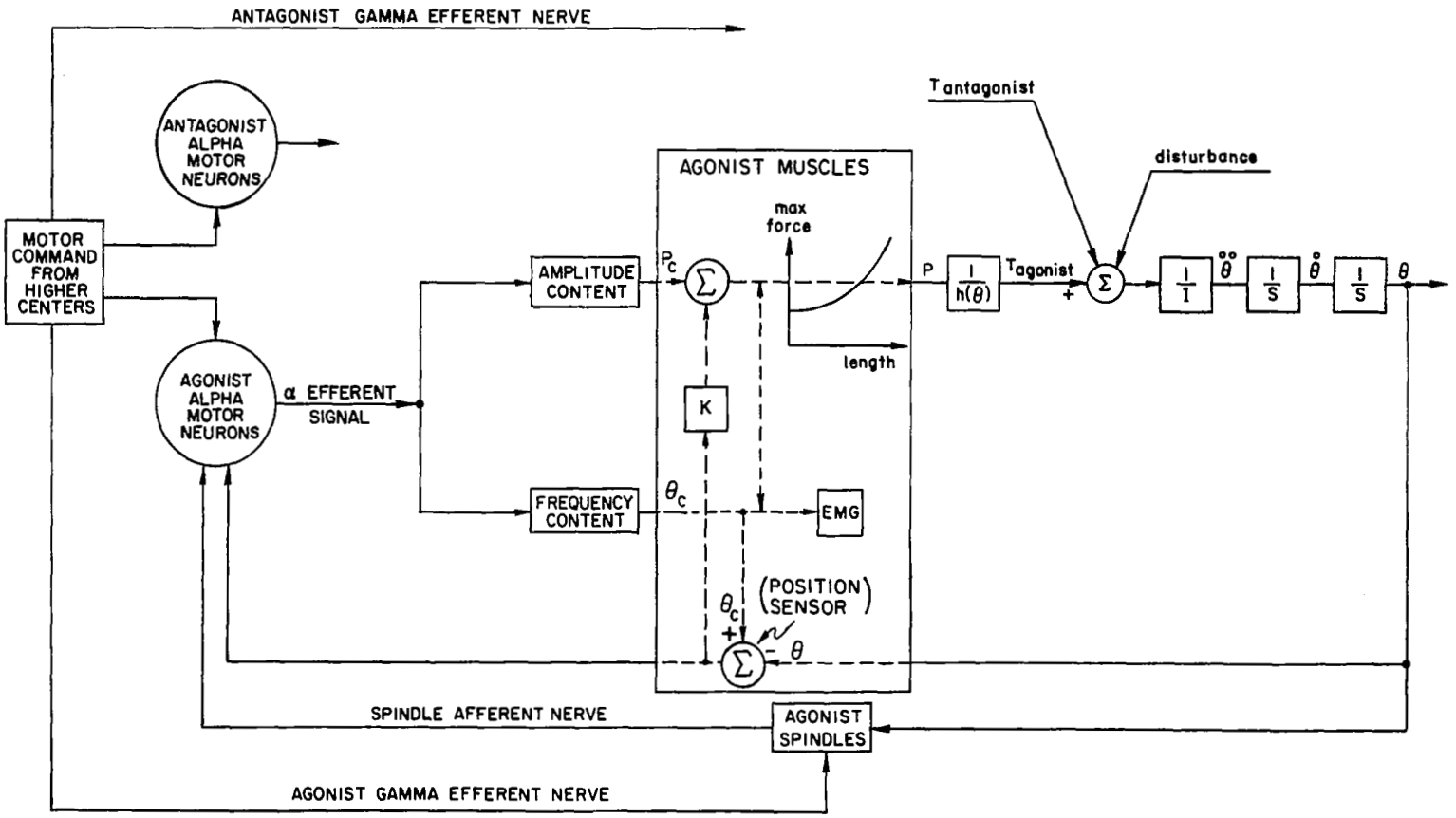

Fig. 40. CONTROL OF MOVEMENT HYPOTHESIS FOR DISSOCIATED FUNCTIONS FOR AMPLITUDE AND FREQUENCY CONTENTS OF HIGHER CENTER MOTOR COMMANDS.

As pointed out by Alter [Ref. 16], it is questionable whether any direct feedback of force information from sensory organs to a conscious level exists. For example, when a constant tension is applied to a spring balance, without using visual feedback, a rapid and wide drift in the force applied will occur.

The system representation of Fig. 40 also indicates the "bounds" or "limits" on the maximum force that can be developed as a function of muscle length. The means by which this constraint on maximum force would enter the voluntary control of movement can be described by considering a limb motion under a high-frequency command from the higher centers and under a large external load P_1. High-frequency excitation implies a large amount of muscle contraction to a final length denoted by x_2. If the maximum force P_2 that can be developed at muscle length x_2 [given by the translational transformation of Eq. (6.18) or (6.19)] is smaller than P_1, however, the motion would stop short of its target x_2 at a larger muscular length x_1, where the maximum developed force is P_1. This is precisely what took place in our isotonic experiments under high-stimulus frequency (tetanic).

A dotted line in the muscle block indicates some influence of discharge frequency on force (no more than 10 to 15 percent according to Leifer) and also shows that EMG is solely a function of total excitation (frequency and amplitude) and not of muscle force alone, except in the isometric case. The function $1/h(\theta)$ is the geometrical transformation converting force to torque, and I is the moment of inertia of the moving limb and load.

The above hypothesis considers the muscle force as the primary parameter in the control of movement. It somewhat reflects an argument (one of many) proposed by Evarts that "neurons related to movement must a priori be related to force--that since the force causes movement, it is unthinkable for PTN's to be related to displacement without first being related to force."

It is emphasized again that the hypothesis brought forward in this discussion is highly speculative. Conclusions from experiments involving electrical stimulation must be drawn with caution. As Ruch [Ref. 17] points out:

"How the motor cortex functions in voluntary activity cannot be directly learned from electrical stimulation, which is not its natural mode of activation. Therefore, much of the research on the motor cortex has been directed toward questions of localization rather than toward the elucidation of its functions."

E. Future Work

A repetition of the experiments conducted during this investigation under stimulations other than maximal and tetanic seems warranted from several standpoints. As the general equations in their implicit forms [Eqs. (2.1) and (2.2)] for the conceptual model indicate, they are not necessarily limited to tetanically and maximally stimulated muscle. It would be useful to obtain a mathematical model that would account for the changing state of activation of muscles; namely, if the parameter $a(t)$ could be described as a time function, rather than a constant, to encompass asynchronous and nonmaximal motor-nerve excitation. This could provide valuable information for the development and design of bioelectric prosthesis for example, where nerve or muscle signals (EMG) from the amputated limb are used to control the prosthesis. Such experiments also would help to test the hypothesis for the voluntary control of movement, discussed in this chapter, and could shed more light on the command structure and logic that activate our system of nerves and muscles.

Another area of application would be in the artificial stimulation of muscles of patients paralyzed by an upper motor lesion but whose muscles are in a normal state; that is, the existing musculature of the paralyzed limb would be utilized as its controlled actuator. Before this can be done, however, muscle behavior as a function of electrical stimulus under a large spectrum of waveform characteristics must be known in addition to that under maximal amplitudes and tetanic frequencies. The results of such a research effort are worthy of the challenge.

Appendix A

RELATIONSHIPS BETWEEN TRANSLATIONAL AND ROTATIONAL COORDINATES AND COMPUTATION OF MUSCLE-GROUP TORQUE ABOUT THE ELBOW JOINT

If a set of unit vectors $\underline{i}$, $\underline{j}$, $\underline{k}$ (considered fixed in the muscle) is defined as shown in Fig. 41 and if

$x \equiv$ length of muscle group

$d \equiv$ distance between muscle-group attachment point at forearm and elbow joint

$\ell \equiv$ distance between muscle-group attachment point at shoulder and elbow joint

$\underline{P} \equiv$ tension vector in muscle

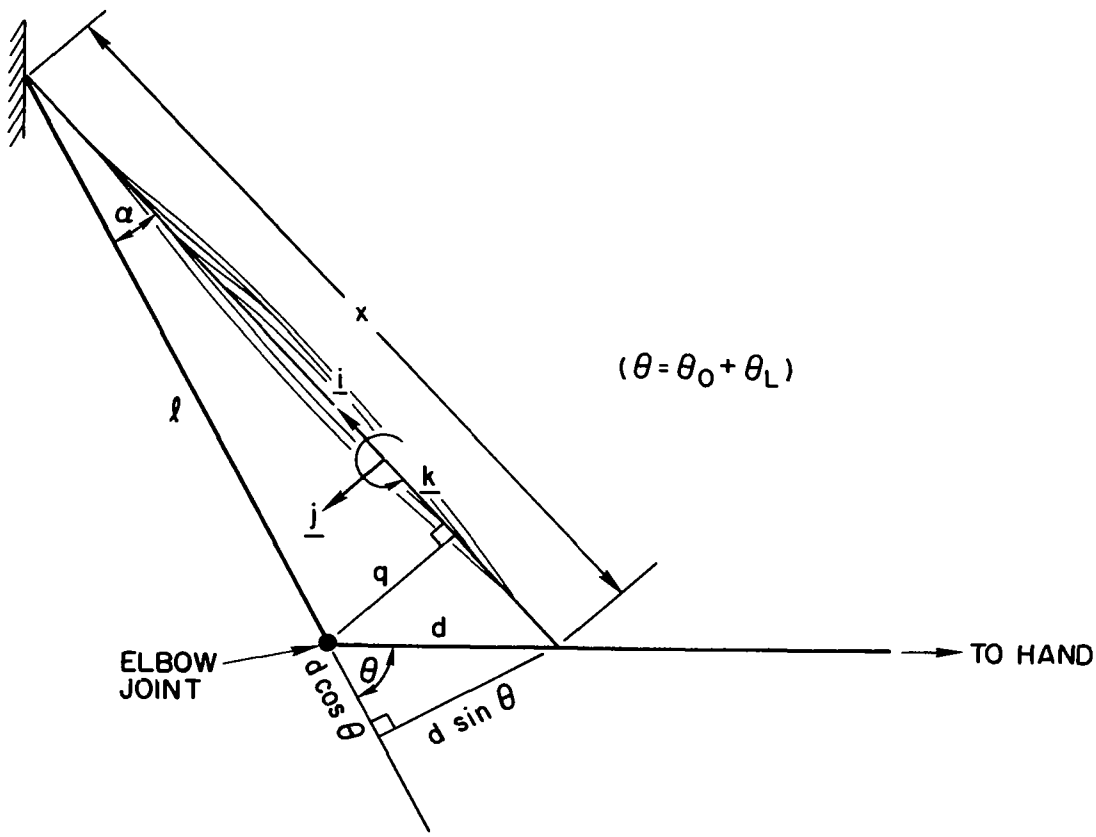

Fig. 41. GEOMETRIC REPRESENTATION OF ARM/MUSCLE-GROUP SYSTEM.

$\underline{T_A}$ ≡ muscle-group torque vector about elbow

$\underline{q}$ ≡ moment arm vector of muscle force about elbow joint

and angles α and θ are defined as indicated in Fig. 41, then the following relationships can be written:

$$x^2 = (\ell + d \cos \theta)^2 + (d \sin \theta)^2$$

or

$$x = (\ell^2 + d^2 + 2\ell d \cos \theta)^{1/2} \tag{A.1}$$

and, for the definitions of x_C, x_L, θ_0, θ_C, and θ_L in Chapter III,

$$\underline{x_C} = \left(\ell^2 + d^2 + 2\ell d \cos \theta_0\right)^{1/2} - \left[\ell^2 + d^2 + 2\ell d \cos (\theta_0 + \theta_C)\right]^{1/2} \underline{i} \tag{A.2}$$

and

$$\underline{\dot{x}_C} = \frac{\ell d \sin (\theta_0 + \theta_C)}{\left[\ell^2 + d^2 + 2\ell d \cos (\theta_0 + \theta_C)\right]^{1/2}} \dot{\theta}_C \underline{i} \tag{A.3}$$

Similarly,

$$\underline{x_L} = \left(\ell^2 + d^2 + 2\ell d \cos \theta_0\right)^{1/2} - \left[\ell^2 + d^2 + 2\ell d \cos (\theta_0 + \theta_L)\right]^{1/2} \underline{i} \tag{A.4}$$

$$\underline{\dot{x}_L} = \frac{\ell d \sin (\theta_0 + \theta_L)}{\left[\ell^2 + d^2 + 2\ell d \cos (\theta_0 + \theta_L)\right]^{1/2}} \dot{\theta}_L \underline{i} \tag{A.5}$$

Now,

$$\underline{q} = -\ell \sin \alpha \underline{j} = -\frac{\ell d \sin \theta}{x} \underline{j}$$

and use of Eq. (A.1) yields

$$\underline{q} = \frac{-\ell d \sin \theta}{\left(\ell^2 + d^2 + 2\ell d \cos \theta\right)^{1/2}} \underline{j} \tag{A.6}$$

By definition, the torque of the muscle group about the elbow is

$$\underline{T_A} = \underline{q} \times \underline{P}$$

and because $\underline{P} = P\underline{i}$ and $\theta = \theta_0 + \theta_L$,

$$\underline{T_A} = \frac{P\ell d \sin (\theta_0 + \theta_L)}{\left[\ell^2 + d^2 + 2\ell d \cos (\theta_0 + \theta_L)\right]^{1/2}} \underline{k} \tag{A.7}$$

By noting that θ_0 is a constant and making use of the above results, Eqs. (A.2), (A.3), (A.4), (A.5), and (A.7) can be represented in general forms as

$$x_C = h_1(\theta_C) \tag{A.8}$$

$$\dot{x}_C = \dot{\theta}_C h_2(\theta_C) \tag{A.9}$$

$$x_L = h_3(\theta_L) \tag{A.10}$$

$$\dot{x}_L = \dot{\theta}_L h_4(\theta_L) \tag{A.11}$$

and

$$P = T_A h_5(\theta_L) \tag{A.12}$$

where

$$h_5(\theta_L) = \frac{\left[\ell^2 + d^2 + 2\ell d.\cos (\theta_0 + \theta_L)\right]^{1/2}}{\ell d \sin (\theta_0 + \theta_L)} \tag{A.13}$$

Appendix B

EVALUATION OF THE APPROXIMATION

The general form of the equation characterizing the series elastic element is quite complex:

$$\left[\ell^2 + d^2 + 2\ell d \cos(\theta_0 + \theta_L)\right]^{1/2} - \left[\ell^2 + d^2 + 2\ell d \cos(\theta_0 + \theta_C)\right]^{1/2}$$

$$= f_1(P) \tag{2.5}$$

where the mathematical expression for θ_C is an elliptic integral [see Eq. (6.13)]. In the above form, the value and usefulness of Eq. (2.5) as a mathematical model for the series elastic element become questionable because of its complexity. For this reason, its left-hand side is approximated to the simpler linear form of

$$d(\theta_C - \theta_L) = f_1(P) \tag{B.1}$$

If the following definition is made,

$$\frac{f_1(P)}{d} \triangleq g_1(P) \tag{B.2}$$

Eq. (B.1) can be expressed in the general form of Eq. (2.6) which is the characterization of the series elastic element considered in this study, namely

$$\theta_C - \theta_L = g_1(P) \tag{2.6}$$

Figure 42 is a graphic illustration of the muscle lengths involved in the above approximation, where

$$Q_i \triangleq \left[\ell^2 + d^2 + 2\ell d \cos(\theta_0 + \theta_i)\right]^{1/2} \qquad i = C, L$$

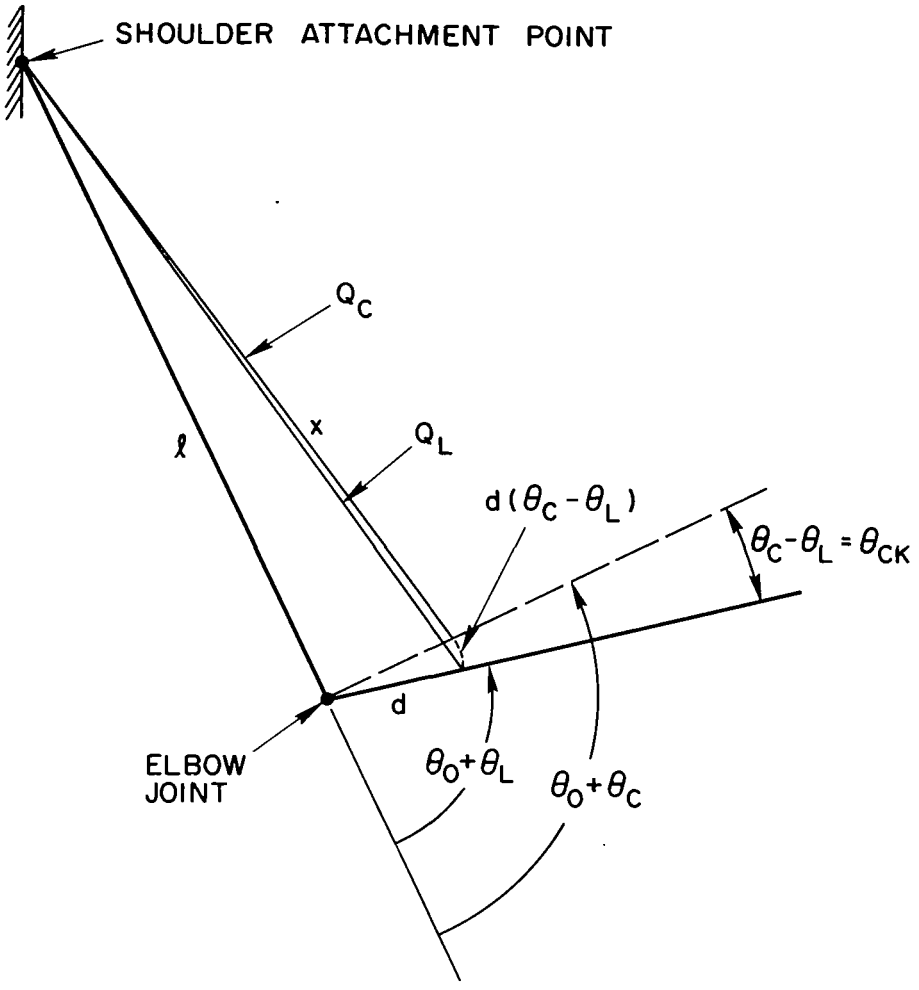

Fig. 42. MUSCLE LENGTHS INVOLVED IN THE APPROXIMATION.

In this notation, the scalar $Q_L - Q_C$ is approximated by $d(\theta_C - \theta_L)$. A numerical evaluation of this approximation for combinations of values assumed by θ_C and θ_L is presented in Table 7, where

$$\% \text{ error} = \frac{\left[d(\theta_C - \theta_L) - (Q_L - Q_C)\right]100}{Q_L - Q_C}$$

The "bounds" for the values of θ_L and θ_C considered in this evaluation are determined by physical constraints.

Table 7

EVALUATION OF ERROR FOR THE APPROXIMATION†

% Error					
$\theta_C - \theta_L$ (deg)	$\theta_0 + \theta_L$ (deg)				
	60	75	90	105	120
5	9.9	2.7	0.9	0.1	4.9
10	9.3	5.7	0.3	2.6	9.8
25	8.7	3.9	1.7	5.1	---
40	7.9	3.4	3.6	---	---
55	6.6	4.3	---	---	---
70	6.7	---	---	---	---

† $d = 2$ in.; $\theta_0 = 40°$; $\ell = 10$ in.;

$$\% \text{ error} = \frac{\left[d(\theta_C - \theta_L) - (Q_L - Q_C)\right]100}{Q_L - Q_C}$$

Lower Bounds: As indicated in Chapter III, the postulated model implies an instantaneous velocity of the forearm at the onset of motion (see Figs. 4 and 5). Because this cannot occur physically, the data collected for the initial part of the forearm motion ($40° \leq \theta_0 + \theta_L < 60°$) were not used to describe the model; therefore, the lowest value of interest for $\theta_0 + \theta_L$ is 60°. By the definitions‡ of θ_C and θ_L, it is clear that the lower bound for $\theta_0 + \theta_C$ at any instant is the value of $\theta_0 + \theta_L$ at the same instant.

‡ $\theta_C = \theta_L + \theta_{CK}$ and $\theta_{CK} > 0$.

Upper Bounds: The largest forearm flexions considered corresponded to $\theta_0 + \theta_L = 120°$. Beyond this value, the upper arm interferes with the forearm movement as actual contact between them occurs. On the basis of this same geometrical constraint, the upper bound for the value of $\theta_0 + \theta_C$ must be greater than 120° (the upper bound for $\theta_0 + \theta_L$), and 130° was the value considered in Table 7. It should be observed, however, that this upper bound for $\theta_0 + \theta_C$ is purely arbitrary (as long as it is larger than 120°) because $\theta_0 + \theta_C$ cannot be observed.

Other sources of errors that have not been considered in this investigation are the following.

(1) The actual attachment points of the biceps and brachialis at the shoulder and arm do not coincide and lead to a more complex arm/muscle geometry than the one assumed.

(2) The elbow joint is not a pure "pin" joint as the one assumed but has some "sliding" characteristics.

(3) Friction at the elbow and electric motor shaft were neglected.

In the light of these errors, those presented in Table 7 are not likely to affect significantly our mathematical models in their final forms.

REFERENCES

1. A. V. Hill, "The Heat of Shortening and the Dynamic Constants of Muscle," Proc. Roy. Soc., B, 126, 1938, pp. 136-195.

2. D. T. McRuer and E. Krendel, "Dynamic Response of Human Operators," WADC TR 56-524, 1957. DDC No. AD 110 693

3. A. Levin and J. Wyman, "The Viscous Elastic Properties of Muscle," Proc. Roy. Soc., B., 101, 1927, pp. 218-243.

4. F. E. Zajac, "The Mathematical Formulation of the Kinematic Properties of Muscle Derived from an Experimental Investigation," Ph.D. dissertation, Stanford University, Stanford, Calif., 1968.

5. L. Vodovnik, W. J. Crochetiere, and J. B. Reswick, "Control of a Skeletal Joint by Electrical Stimulation of Antagonists," Med. and Biol. Engineering, 5, 1967, pp. 97-109.

6. L. J. Leifer, "Characterization of Single Muscle Fiber Discharge during Voluntary Isometric Contraction of the Biceps Brachii Muscle in Man," Ph.D. dissertation, Stanford University, Stanford, Calif., 1969.

7. J. M. Ritchie and D. R. Wilkie, "The Dynamics of Muscular Contraction," J. Physiol., 143, 1958, pp. 104-113.

8. A. V. Hill, "Water and Heat in a Muscle Twitch," Proc. Roy. Soc., B., 136, 1949, pp. 220-228.

9. A. V. Hill, "The Abrupt Transition from Rest to Activity in Muscle," Proc. Roy. Soc., B., 136, 1949, pp. 399-420.

10. B. C. Abbott and D. R. Wilkie, "The Relation between Velocity of Shortening and the Tension-Length Curve of Skeletal Muscle," J. Physiol., 117, 1953, pp. 77-86.

11. B. R. Jewell and D. R. Wilkie, "An Analysis of the Mechanical Components in Frog's Striated Muscle," J. Physiol., 143, 1958, pp. 515-540.

12. F. D. Carlson, "Kinematic Studies on Mechanical Properties of Muscle," in Tissue Elasticity (J. W. Remington, ed.), Am. Physiol. Soc., Washington, D.C., 1957.

13. W. O. Fenn and B. S. Marsh, "Muscular Force at Different Speeds of Shortening," J. Physiol., 85, 1935, pp. 277-297.

14. E. V. Evarts, "Relation of Pyramidal Tract Activity to Force Exerted during Voluntary Movement," J. Neurophysiol., 1967.

15. L. D. Partridge, "Signal-Handling Characteristics of Load-Moving Skeletal Muscle," Am. J. Physiol., 5, 210, 1966, pp. 1178-1191.

16. R. Alter, "Bioelectric Control of Prostheses," MIT Research Lab. of Electronics, TR No. 446, Cambridge, Mass., 1966.

17. T. G. Ruch, "Motor Systems," in Handbook of Experimental Psychology, (S. S. Stevens, ed.), John Wiley & Sons, New York, 1951, pp. 154-208.

18. D. T. McRuer et al, "Human Pilot Dynamics in Compensatory Systems--Theory, Models, and Experiments with Controlled Element and Forcing Function Variations," AFFDL, TR No. 65-15, 1965. DDC No. AD 470 337

19. D. T. McRuer, R. E. Magdaleno, and G. P. Moore, "A Neuromuscular Actuation System," USC-NASA Conf. on Manual Control, 1967.

20. W. J. Crochetiere, L. Vodovnik, and J. B. Reswick, "Electrical Stimulation of Muscle--A Study of Muscle as an Actuator," Med. and Biol. Engineering, 5, 1967, pp. 111-125.

21. D. T. Greenwood, Principles of Dynamics, Prentice-Hall, Inc., New Jersey, 1965.

22. B. Katz, "The Relation between Force and Speed in Muscular Contraction," J. Physiol., 96, 1939, pp. 45-64.

23. B. Bigland and O. C. J. Lippold, "The Relation between Force, Velocity, and Integrated Electrical Activity in Human Muscles," J. Physiol., 123, 1954, pp. 214-224.

24. D. R. Wilkie, "The Mechanical Properties of Muscle," Brit. Med. Bull., 3, 12, 1958, pp. 177-182.

25. X. Aubert, "Le Couplage Energetique de la Contraction Musculaire," thèse d' agrégation, Brussels, 1956.

26. C. R. Dorf, Modern Control Systems, Addison-Wesley Series in Electrical Engineering, 1967.

27. J. E. Gibson, Nonlinear Automatic Control, McGraw-Hill Book Co., New York, 1963.

28. B. Katz, Nerve, Muscle, and Synapse, McGraw-Hill Series in New Biology, 1966.

29. H. T. Milhorn, The Application of Control Theory to Physiological Systems, W. B. Saunders and Co., Philadelphia, 1966.

30. T. G. Ruch and H. D. Patton, Physiology and Biophysics, W. B. Saunders and Co., Philadelphia, 1965.

NASA-Langley, 1970 — 4 CR-1691